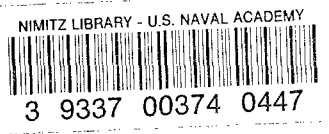ad 772 098

NAVAL SHIP RESEARCH AND DEVELOPMENT CENTER
Bethesda, Maryland 20034

FORCE AND MOMENT CHARACTERISTICS OF SIX HIGH-SPEED

RUDDERS FOR USE ON HIGH-PERFORMANCE CRAFT

by

D. L. Gregory

APPROVED FOR PUBLIC RELEASE: DISTRIBUTION UNLIMITED

20070122045

SHIP PERFORMANCE DEPARTMENT
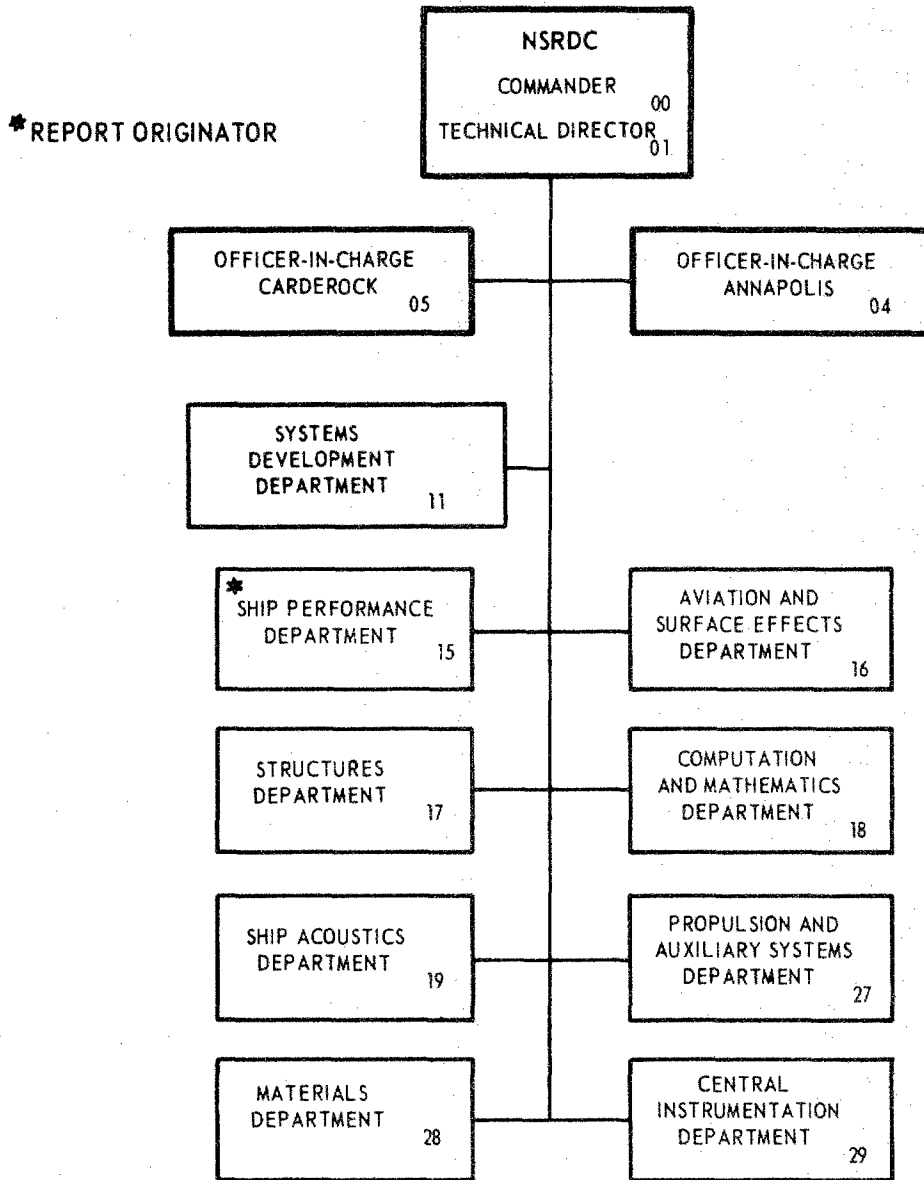RESEARCH AND DEVELOPMENT REPORT

November 1973   Report 4150

MAJOR NSRDC ORGANIZATIONAL COMPONENTS

*REPORT ORIGINATOR

NSRDC
COMMANDER 00
TECHNICAL DIRECTOR 01

OFFICER-IN-CHARGE CARDEROCK 05

OFFICER-IN-CHARGE ANNAPOLIS 04

SYSTEMS DEVELOPMENT DEPARTMENT 11

*SHIP PERFORMANCE DEPARTMENT 15

AVIATION AND SURFACE EFFECTS DEPARTMENT 16

STRUCTURES DEPARTMENT 17

COMPUTATION AND MATHEMATICS DEPARTMENT 18

SHIP ACOUSTICS DEPARTMENT 19

PROPULSION AND AUXILIARY SYSTEMS DEPARTMENT 27

MATERIALS DEPARTMENT 28

CENTRAL INSTRUMENTATION DEPARTMENT 29
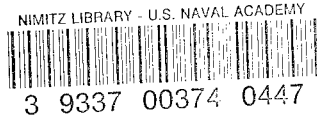
NAVAL SHIP RESEARCH AND DEVELOPMENT CENTER

Bethesda, Maryland 20034

FORCE AND MOMENT CHARACTERISTICS OF SIX HIGH-SPEED

RUDDERS FOR USE ON HIGH-PERFORMANCE CRAFT

by

D. L. Gregory

APPROVED FOR PUBLIC RELEASE: DISTRIBUTION UNLIMITED

20070122.045

SHIP PERFORMANCE DEPARTMENT

RESEARCH AND DEVELOPMENT REPORT

November 1973

Report 4150

DEPARTMENT OF THE NAVY

NAVAL SHIP RESEARCH AND DEVELOPMENT CENTER

BETHESDA, MD. 20034

FORCE AND MOMENT CHARACTERISTICS OF SIX HIGH-SPEED

RUDDERS FOR USE ON HIGH-PERFORMANCE CRAFT

by

D. L. Gregory

APPROVED FOR PUBLIC RELEASE: DISTRIBUTION UNLIMITED

November 1973   Report 4150

TABLE OF CONTENTS

LIST OF FIGURES

NOTATION

Symbol	Definition	Dimensions
A	Aspect ratio b^2/S	
b	Span measured perpendicular to the plane of the root section	feet
$\overline{c}$	Mean geometric chord, $(\text{Chord}_{tip} + \text{Chord}_{root})/2$	feet
C_D	Drag coefficient, $D/\frac{1}{2}\rho S V^2$	
C_L	Lift coefficient, $L/\frac{1}{2}\rho S V^2$	
$C_{M_{C/4}}$	Torque coefficient about the mean geometric quarter chord, $M_C/\frac{1}{2}\rho S\overline{c}V^2$	
D	Drag parallel to flow	pound
g	Acceleration due to gravity	feet per square second
L	Lift normal to direction of flow	pound
M_C	Rudder stock torque	pound-feet
M_b	Rudder stock bending moment	pound-feet
P_s	Static pressure	pounds per square foot
P_v	Vapor pressure	pounds per square foot
R_e	Reynolds number $V\overline{c}/\nu$	
S	Rudder planform area	square feet

Symbol	Definition	Dimensions
V	Velocity of free stream	feet per second
α	Rudder angle (angle of attack)	degrees
ν	Kinematic viscosity	square feet per second
ρ	Mass density	pound-square second per feet^4
σ	Cavitation number $(P_s - P_v)/\frac{1}{2}\rho V^2$	

ABSTRACT

Six rudders with a geometric aspect ratio of 1.5 and widely varying section shapes were constructed to determine the effect of section shape on the cavitating performance of high-speed rudders. Experiments were conducted in the 24-in. variable-pressure water tunnel at cavitation indices between 4.0 and 0.5 and an angle of attack range from -5 to +35 deg. Section shape had little effect on the lift curve slope or on the maximum lift coefficient. However, the blunt base sections had substantially higher drag coefficients throughout the normal operating range of rudder angles. Rudder stock torque was significantly affected by section shape and cavitation index.

ADMINISTRATIVE INFORMATION

INTRODUCTION

The increasing cost of naval ships in the last decade has heightened interest in small high-performance craft, particularly for coastal and inshore warfare. The resultant demand for higher performance, better handling, and improved motion characteristics in a seaway has created a need for better predictions of speed and power, turning and maneuvering, and motion for such craft. This investigation of high-performance craft rudders is intended to provide much needed information on the force characteristics of rudders under the cavitating conditions experienced by high-performance craft. The purpose of this report is to aid in the design of rudders and steering gear and to provide rudder force characteristics for turning and maneuvering predictions.

A geometric aspect ratio of 1.5 was selected as representative of the current trend in rudder design. The two parameters chosen as variables were rudder section shape and cavitation number.

THE RUDDER SERIES

Rudder profiles and typical section shapes for the six rudders
tested are shown in Figures 1-6. The rudders were constructed of brass and
polished to a smooth finish. They were fitted with 5/8-in. stainless steel
stocks located at the mean quarter-chord point. All had a span of 7.5 in.
and a mean chord of 5.0 in.; this gave a geometric aspect ratio of 1.5 and
a projected area of approximately 37.5 in^2. Since Rudders 2, 3, and 5 had
very thin leading edges, it was necessary to increase the width at the root
so that it was thick enough to house the rudder stock. The normal rudder
sections were maintained to a point 1 in. below the root on the model;
above this point, the sections were thickened near the leading edge and
were faired into the root section. This fairing is illustrated in Figures
2, 3, and 5.

METHOD AND PROCEDURE

The experiments were conducted in the NSRDC 24-in. variable-pressure
water tunnel.[1] The rudder angle was varied from -5 to +35 deg in 5-deg
increments. The tunnel pressure and velocity were set to correspond to
cavitation indices of 4.0, 2.0, 1.5, 1.0, and 0.5 for each rudder angle.
A water velocity of 23 ft/sec for cavitation indices of 4.0 through 1.0
corresponds to a Reynolds number of approximately 1.02×10^6. The tunnel
velocity was increased to 25 ft/sec for the 0.5 cavitation index, resulting
in a small (about 8 percent) increase in Reynolds number for this condition
compared to the other cavitation indices. The lower velocity at higher
cavitation numbers was necessitated by the capacity of the force balance.
Table 1 summarizes the experimental conditions. The cavitation patterns
were observed and sketched for each condition.

---

[1]Brownell, W. F. and M. L. Miller, "Hydromechanics Cavitation Research
Facilities and Techniques in Use at the David Taylor Model Basin," David
Taylor Model Basin Report 1856 (Oct 1964).

2

TABLE 1 - SUMMARY OF EXPERIMENTAL CONDITIONS FOR EACH RUDDER

(Superscript numbers indicate the rudders on which cavitation first appeared for the indicated test condition)

Angle of Attack deg	σ	Tunnel Velocity ft/sec	Angle of Attack deg	σ	Tunnel Velocity ft/sec
-5	4.0	23	20	4.0	23
	2.0			2.0[1,2]	
	1.5			1.5	
	1.0			1.0	
	0.5	25		0.5	25
0	4.0	23	25	4.0	23
	2.0			2.0	
	1.5			1.5	
	1.0			1.0	
	0.5	25		0.5	25
5	4.0	23	30	4.0	23
	2.0			2.0	
	1.5			1.5	
	1.0[3,4,6]			1.0	
	0.5[2-6]	25		0.5	25
10	4.0	23	35	4.0	23
	2.0[3-6]			2.0	
	1.5[2-6]			1.5	
	1.0[5]			1.0	
	0.5[1]	25		0.5	25
15	4.0	23			
	2.0[2]				
	1.5[1]				
	1.0[1]				
	0.5	25			

The rudders were tested below an 8.0-in. × 21.5-in. aluminum plate with a gap of approximately $0.005\overline{c}$ between the top of the rudder and the plate. Forces and moments were measured with four 2-in. modular force gages and with a transmission dynamometer mounted above the plate and housed in a faired strut. A schematic diagram of the measurement system is shown in Figure 7. All gages were calibrated individually, assembled in the system, and then calibrated as a total system. Lift and drag forces are accurate to ±0.5 lb, rudder stock torque to ±0.5 in-lb, and rudder stock bending moments to ±1.0 in-lb. Lift forces on the model rudders varied from 0 to 150 lb, and the drag varied from near zero to approximately 75 lb. Maximum rudder stock torques were in the order of 100 in-lb.

All data were reduced to nondimensional coefficient forms compatible with the coefficients presented by Whicker and Fehlner.[2]

RESULTS AND DISCUSSION

Figures 8-13 show representative cavitation patterns for the six rudders, and Figures 14-19 indicate their lift, drag, and torque coefficients. Figure 20 presents a comparison of the lift and drag coefficients of the six rudders at σ = 4.0 and 0.5. It is apparent from Figures 14-19 that the NACA 0015 section rudder (Rudder 1) was the only one that showed any appreciable loss in maximum lift coefficient for cavitation indices of 1.0 or greater. This deterioration occurred mainly at rudder angles greater than 15 deg; such angles are probably beyond the normal operating range of a high-speed rudder. The effective angle of attack of a rudder operating on a real craft will generally be somewhat less than the rudder angle once the craft starts to turn.

The lift curve slopes $(dC_L/d\alpha)$ of the six rudders for σ = 4.0 and 1.0 did not vary significantly from one another for angles of attack less

---

[2] Whicker, L. F. and L. F. Fehlner, "Free-Stream Characteristics of a Family of Low-Aspect Ratio, All-Movable Control Surfaces for Application to Ship Design," David Taylor Model Basin Report 933 (May 1958).

than 15 deg. The maximum lift occurred between 22 and 25 deg for all rudders except Rudder 6 where the maximum was at approximately 27 deg. Rudders 2, 3, and 5, which had their maximum thickness at the trailing edge, had both higher lift slope and higher maximum lift coefficients than the other three.

The flat plate had the lowest maximum lift coefficient; however, the lift slope was equal to the NACA 0015 section up to an angle of attack of 15 deg. For angles less than 25 deg, the drag of the NACA 0015 section shape rudder was substantially less than that of any of the other five rudders tested. If the lift to drag ratio of a rudder is used as a figure of merit, then the NACA 0015 rudder performed best. This can be seen from Figure 21 which shows a comparison of the L/D ratios of the six rudders for $\sigma = 4.0$ and 0.5. The NACA 0015 rudder exhibited high negative torque on the rudder stock over a wide range of angles. This means that once the rudder started to turn, it would turn further on its own until it reached a high angle of attack. This can be rectified by increasing the sweep angle or moving the rudder stock forward.

Considering manufacturing costs, particularly on a craft of medium speed, the flat plate rudder is probably the best choice. The drag coefficient lies about midway between the high and the low values obtained with this rudder series. The drag coefficient of the flat plate rudder at 0-deg angle of attack could probably be reduced by fairing the trailing edge with straight line sections so that the trailing edge has a 20- to 30-deg included angle.

At high speed ($\sigma = 0.5$), the lift curve slope for the NACA 0015 section was equal to the noncavitating lift curve slope up to approximately 10 deg. Beyond a 10-deg angle of attack, the lift slope dropped sharply and the maximum lift coefficient was in the order of 60 to 70 percent of the maximum lift coefficient developed at cavitation indices of 1.0 and larger. At cavitation indices of 0.5 and below, the NACA 0015 rudder did not perform as well as in the 1.0 to 4.0 range. The lift on this rudder started to drop rather drastically at approximately 18 deg and continued until it reached a minimum at approximately 24 deg. At low angles of attack, however, the drag was still substantially lower than that of any of the other sections tested. At $\sigma = 0.5$, the performance of the flat

plate rudder again suggested that this rudder is a reasonably good selection. However, it is likely that under cavitation conditions, both rudders will have cavitation erosion problems. At $\sigma = 0.5$ and lower, Rudder 2 (the parabolic section) is probably the best choice. Its thicker leading edge will be less subject to damage than Rudders 3 and 5 and it does not require as much thickening to provide adequate strength in the area of the rudder stock. The parabolic section was less susceptible to cavitation erosion damage than the flat plate or the NACA 0015 section.

The effect of cavitation on the lift, drag, and rudder stock torque characteristics has already been discussed. It is interesting to note that cavitation actually began at considerably lower (simulated) speeds than the speed where any detrimental effects in performance were first observed. Unfortunately, cavitation inception studies on these rudders were not conducted; however, cavitation patterns were observed at each test condition. The summary of experimental conditions (Table 1) indicates the point at which cavitation was first observed for each rudder. Since both the cavitation number and the angle of attack were varied in discrete increments, the actual cavitation inception point will probably occur at a higher value of σ than indicated in Table 1. It is shown, for example, that cavitation was first present on Rudder 3 at a 5-deg angle of attack and $\sigma = 1.0$. Since no cavitation was indicated at $\sigma = 1.5$, it can be assumed that the actual inception point for Rudder 3 at a 5-deg angle of attack was between $\sigma = 1.5$ and 1.0.

The stepped rudder (Rudder 6 shown in Figure 6) was designed to operate with the after portion unwetted at high speeds, in order to reduce the drag, but flow separation did not seem to take place. At $\sigma = 0.5$ and a 0-deg angle of attack, a very small cavity in the order of 1/8 in. long formed behind the step. At higher sigma values there was no evidence of cavitation at the step and the drag results do not indicate that flow separation occurred. Since this rudder was designed to operate very near the surface where there is a distinct possibility of ventilation, it was decided to try to ventilate the rudder by injecting air at the step. Air was injected by leading a tube (inside diameter of approximately 3/32 in.) from the bottom of the tunnel. Several locations of the air tube as well as several angles of attack on the rudder were investigated. It was not

possible to ventilate the rudder at the step in this manner, providing further evidence that flow separation was not present. When ventilation did occur, the rudder ventilated from the leading edge. Thus, it was not possible to obtain the characteristics of this rudder with the afterbody unwetted. If it does not ventilate, Rudder 6 offers no significant advantage over Rudders 2, 3, and 5. These experiments are not conclusive proof that the rudder will not ventilate under full-scale conditions.

For this series of rudders, the spanwise center of pressure was between 40 to 50 percent of the span from the root. For the purpose of sizing the rudder stock, the spanwise center of pressure may be assumed to be 0.45b from the root. The rudder stock bending moment may then be calculated as

$$M_B = \sqrt{L^2 + D^2} \times 0.45b$$

COMPARISON WITH OTHER EXPERIMENTAL DATA

The lift and drag coefficients for Rudder 1 (NACA 0015) obtained from this series of experiments are compared in Figures 22 and 23 with data for similar rudders.[2, 3] The water tunnel results from Kerwin et al.[3] are for a rudder with an NACA 66 section of aspect ratio 1.4; they agreed quite well in both lift and drag and with the results obtained here for angles of attack of less than 20 deg. The lift slope of the NACA 66 rudder was slightly lower than for Rudder 1 of the present study; this is what one would expect since the aspect ratio was lower. Figure 23 shows that the drag characteristics of these two rudders began to deviate considerably at angles of attack larger than 20 deg. This lack of agreement between the drag coefficients is due to the difference in stall angles. The lift breakdown occurred at 20 deg on the NACA 66 rudder and at 23 deg on the NACA 0015 rudder.

---

[3]Kerwin, J. E. et al., "An Experimental Study of a Series of Flapped Rudders," Mass. Inst. Technol. Report 71-19 (Jul 1971).

The results of the wind tunnel lift data[2] corrected to a Reynolds number of 1.02×10^6 agreed reasonably well with water tunnel data from the present study. The lift curve slope $\left(dC_L/d\alpha\right)$ obtained in the wind tunnel was 0.0506 compared to 0.0467 for the water tunnel studies. This represents a difference of approximately 10 percent in the lift curve slope. The maximum lift coefficient, however, was about the same for both series of experiments. The drag data in Figure 23 show about a 10-percent difference between the wind tunnel and water tunnel experiments. No corrections for Reynolds number effects were made to the wind tunnel data for the drag coefficient because Whicker and Fehlner[2] had indicated that a change in Reynolds number from 1.02×10^6 to 2.26×10^6 did not significantly affect the drag.

The agreement among the three experiments is quite reasonable. The data presented in this paper are therefore considered sufficiently accurate for use in designing rudders for high-performance craft.

CONCLUSIONS

1. Rudder section shape has little effect on rudder effectiveness (lift curve slope) for angles less than 15 deg.

2. For cavitation number values of 1.0 and larger, Rudder 1 (NACA 0015 section) has the highest lift to drag ratio and the lowest drag.

3. For low- and medium-speed rudders, the flat plate rudder is a good compromise between cost and performance.

4. For high-speed application ($\sigma = 0.5$ or lower), the parabolic section (Rudder 2) appears to be the best choice.
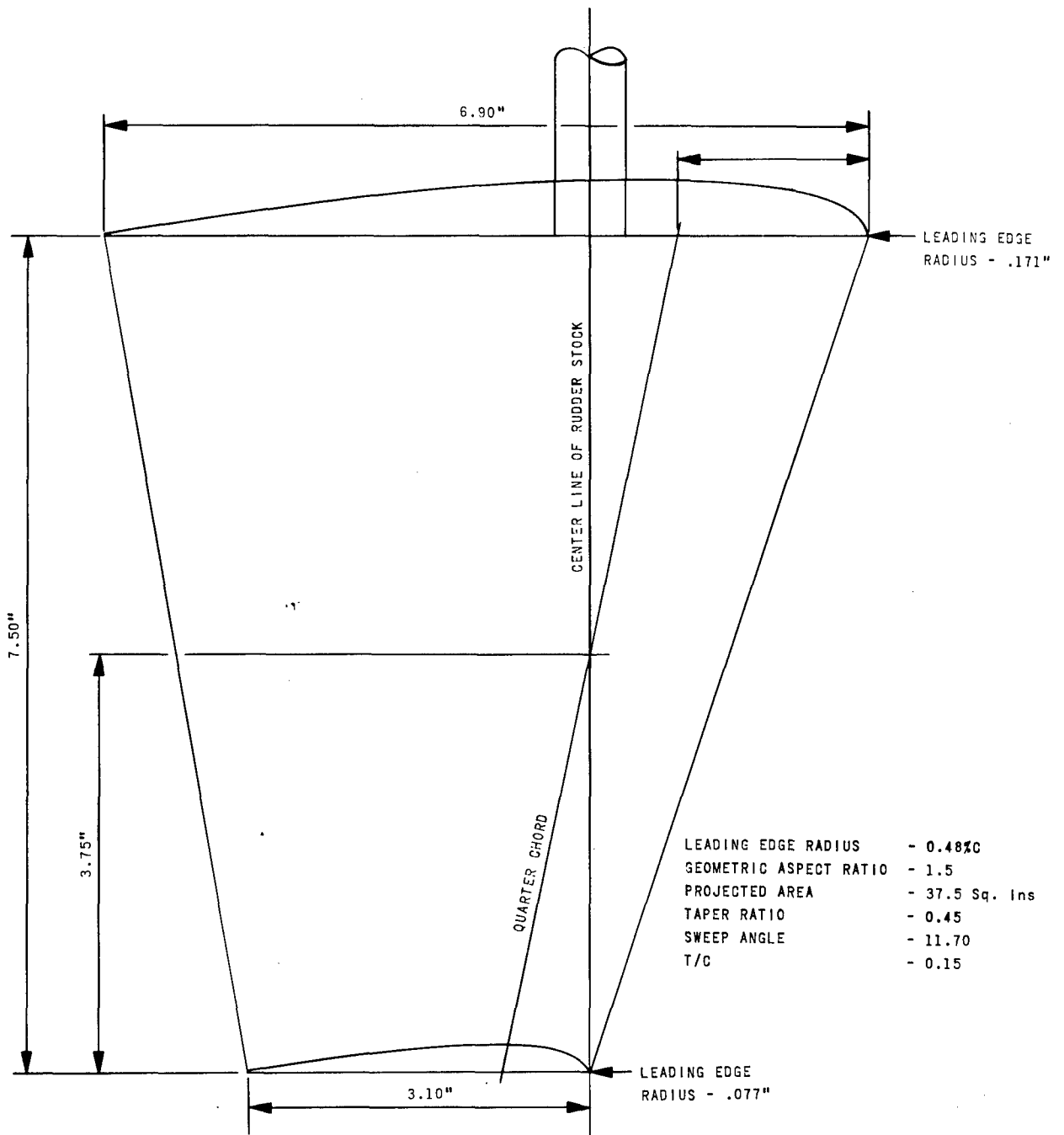
6.90"

LEADING EDGE
RADIUS - .171"

CENTER LINE OF RUDDER STOCK

7.50"

3.75"

QUARTER CHORD

LEADING EDGE RADIUS   - 0.48%C
GEOMETRIC ASPECT RATIO - 1.5
PROJECTED AREA   - 37.5 Sq. Ins
TAPER RATIO   - 0.45
SWEEP ANGLE   - 11.70
T/C   - 0.15

3.10"

LEADING EDGE
RADIUS - .077"

Figure 1 - Planform and Section Details of Rudder 1

6.53"

LEADING EDGE
RADIUS - .022"

ROOT CHORD

1.00"

1" BELOW ROOT

END OF PARABOLIC
SECTION

6.12"

3.75"

7.50"

MID CHORD

CENTER LINE OF RUDDER STOCK

3.75"

LEADING EDGE RADII - .185% OF CHORD
FROM TIP TO 1" BELOW ROOT.
GEOMETRIC ASPECT RATIO - 1.5
PROJECTED AREA----------37.5 Sq. Ins.
TAPER RATIO------------- 0.53
SWEEP ANGLE------------16.5
T/C-------------------- 0.11

LEADING EDGE
RADIUS - .006"

TIP

3.46"
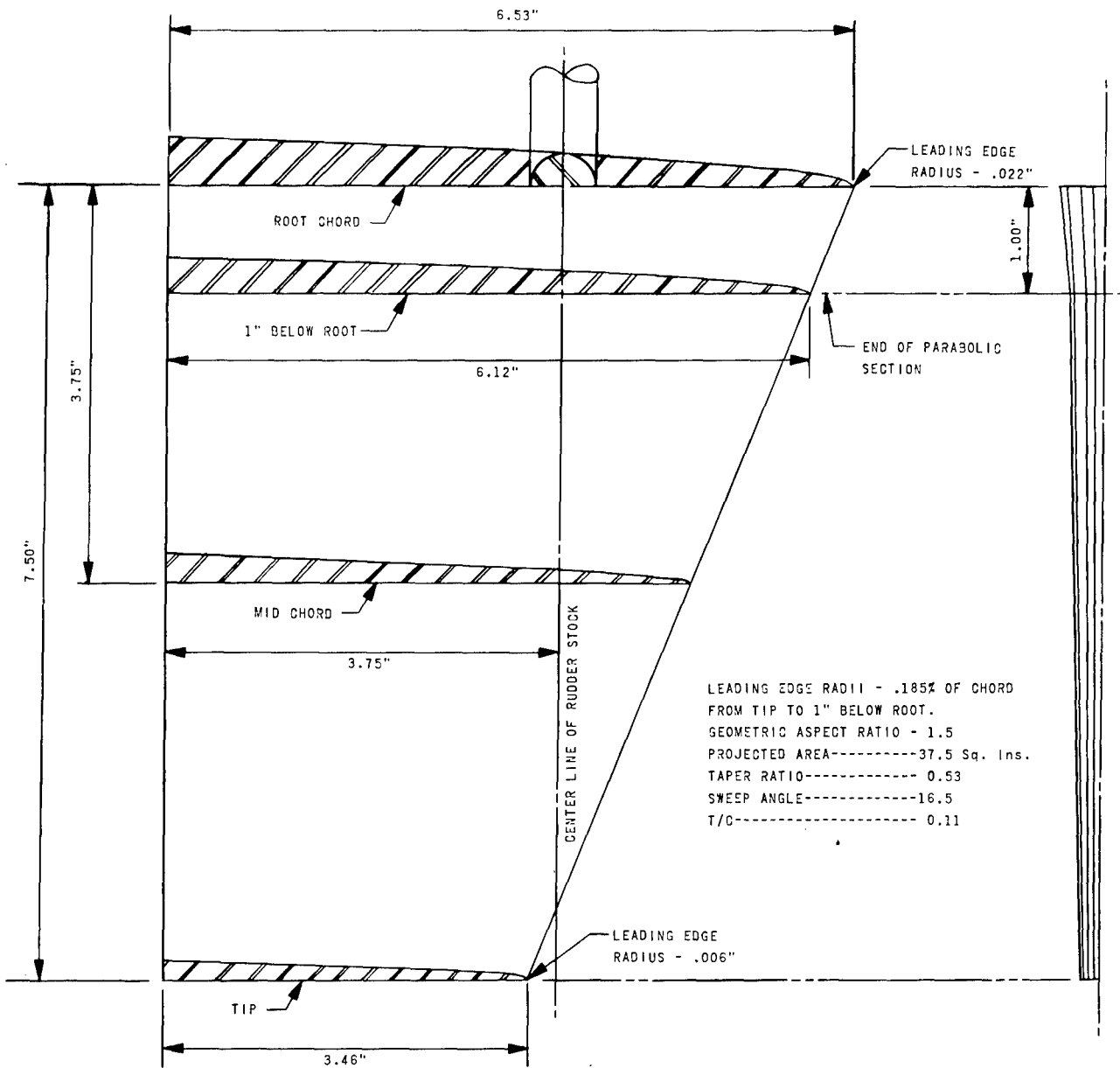
Figure 2 - Planform and Section Details of Rudder 2

10
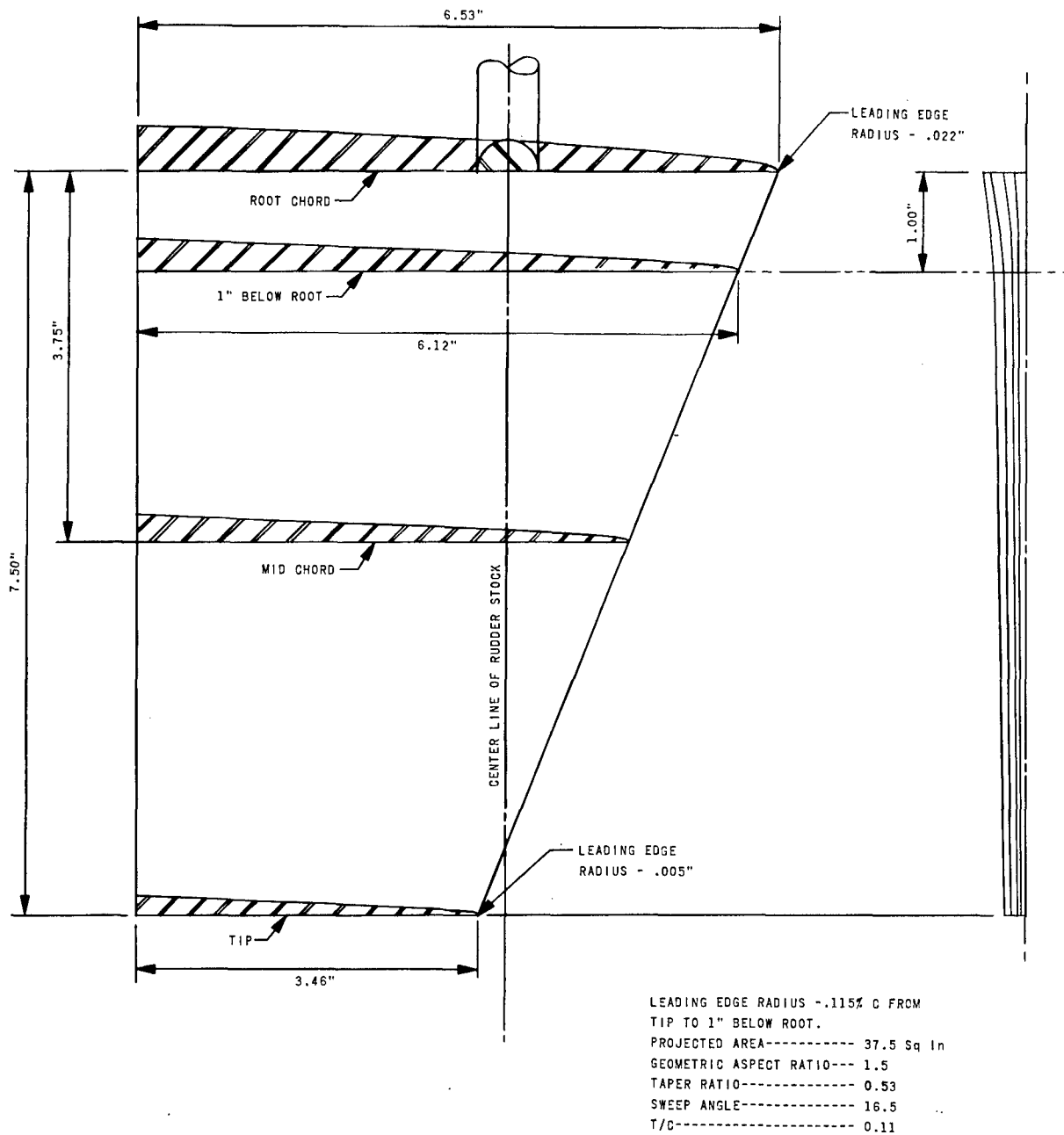
Figure 3 - Planform and Section Details of Rudder 3

The figure contains the following labels and dimensions:

6.53"
LEADING EDGE RADIUS - .022"
1.00"
ROOT CHORD
1" BELOW ROOT
6.12"
3.75"
MID CHORD
7.50"
CENTER LINE OF RUDDER STOCK
LEADING EDGE RADIUS - .005"
TIP
3.46"

LEADING EDGE RADIUS -.115% C FROM
TIP TO 1" BELOW ROOT.
PROJECTED AREA----------- 37.5 Sq In
GEOMETRIC ASPECT RATIO--- 1.5
TAPER RATIO------------- 0.53
SWEEP ANGLE------------- 16.5
T/C--------------------- 0.11
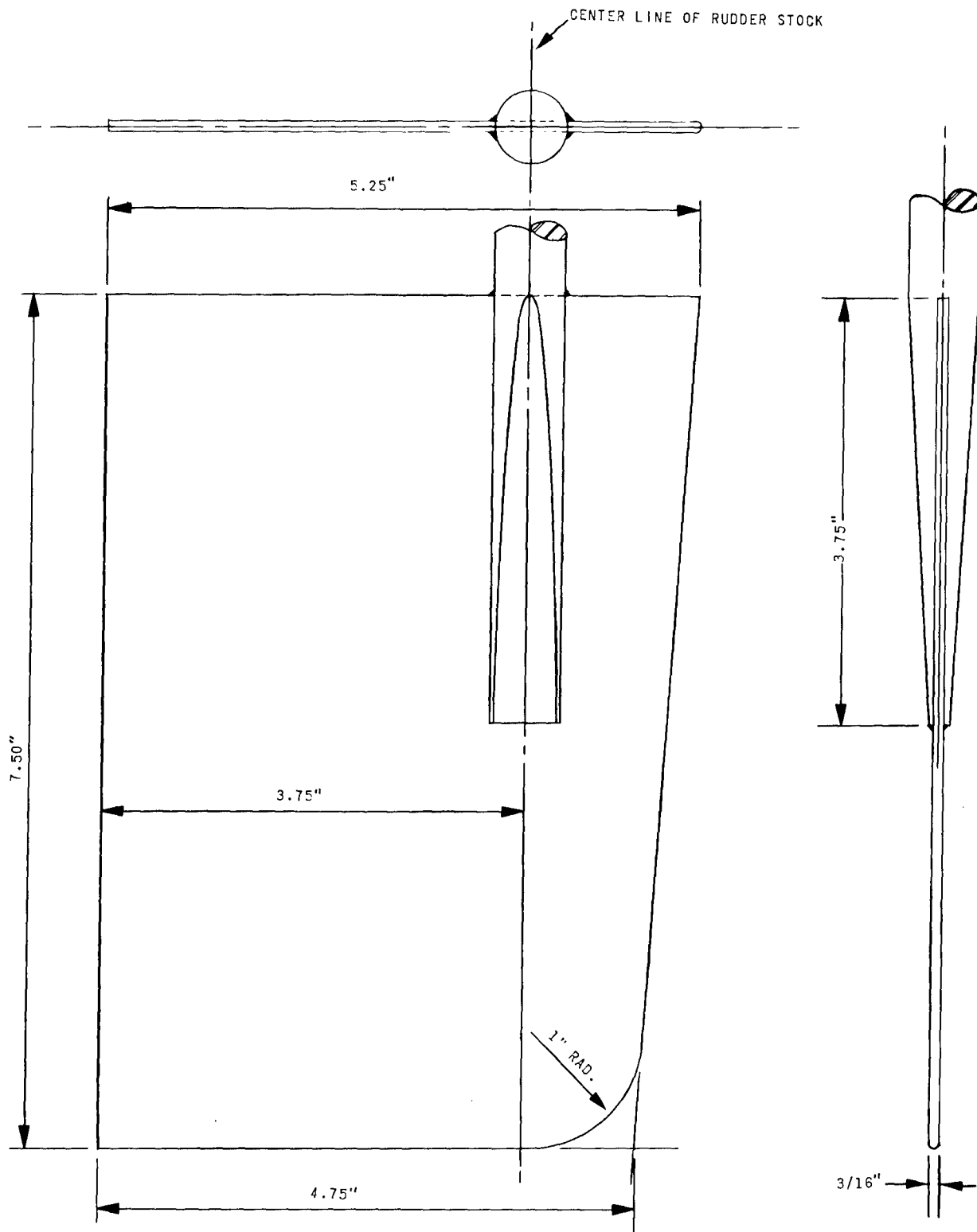
Figure 4 - Planform and Section Details of Rudder 4

Within the figure:

6.53"

ROOT

ROOT -1" — END OF WEDGE SECTION

6.1"

1.00"

3.75"

7.50"

MID CHORD

3.72"

CENTER LINE OF RUDDER STOCK

LEADING EDGE
RADII - 008"

TIP

3.46"

LEADING EDGE .008" RADIUS
GEOMETRIC ASPECT RATIO - 1.5
PROJECTED AREA - 37.5 Sq. Ins.
TAPER RATIO - 0.53
SWEEP ANGLE - 16.5
T/C - 0.11
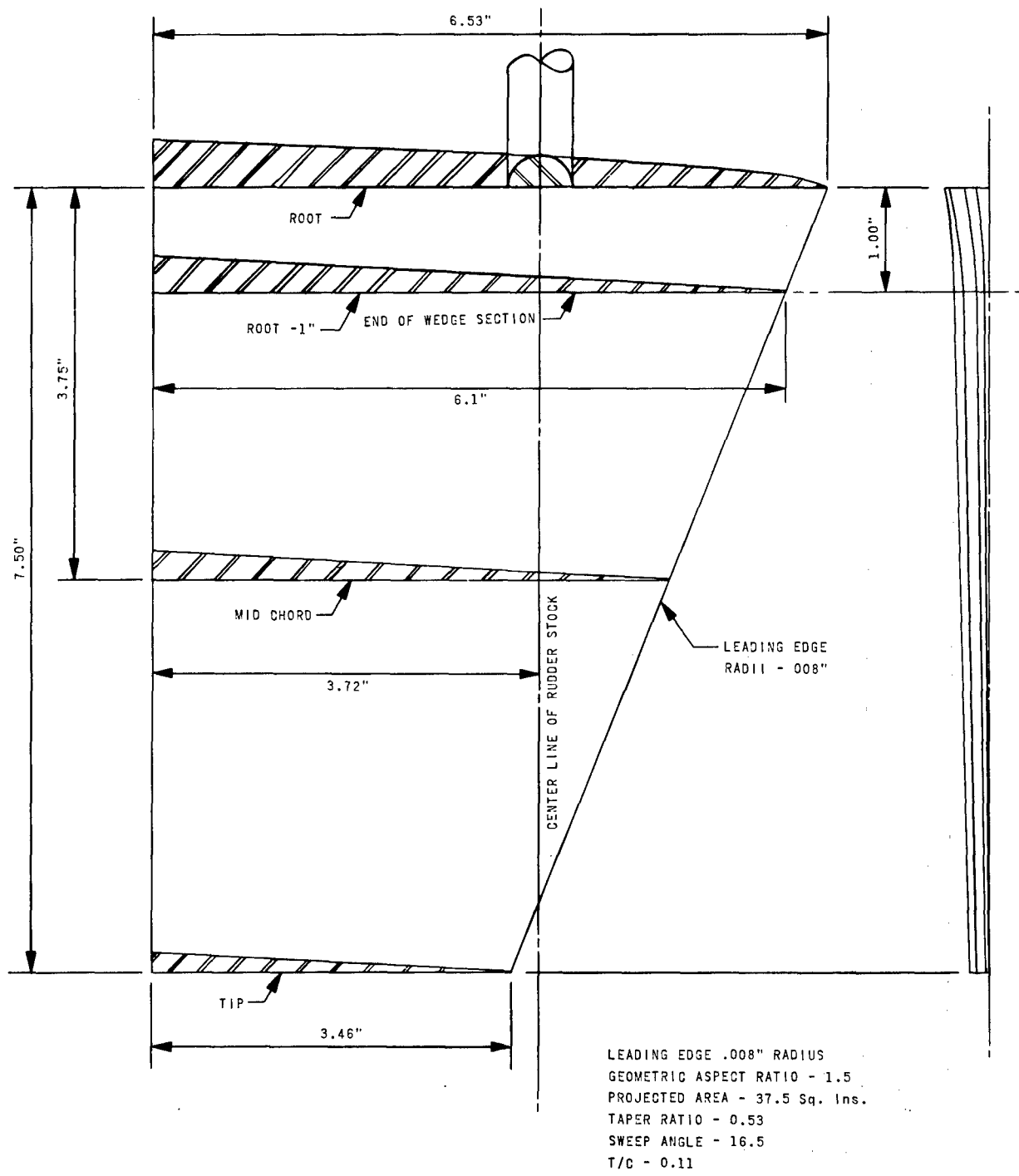
Figure 5 - Planform and Section Details of Rudder 5
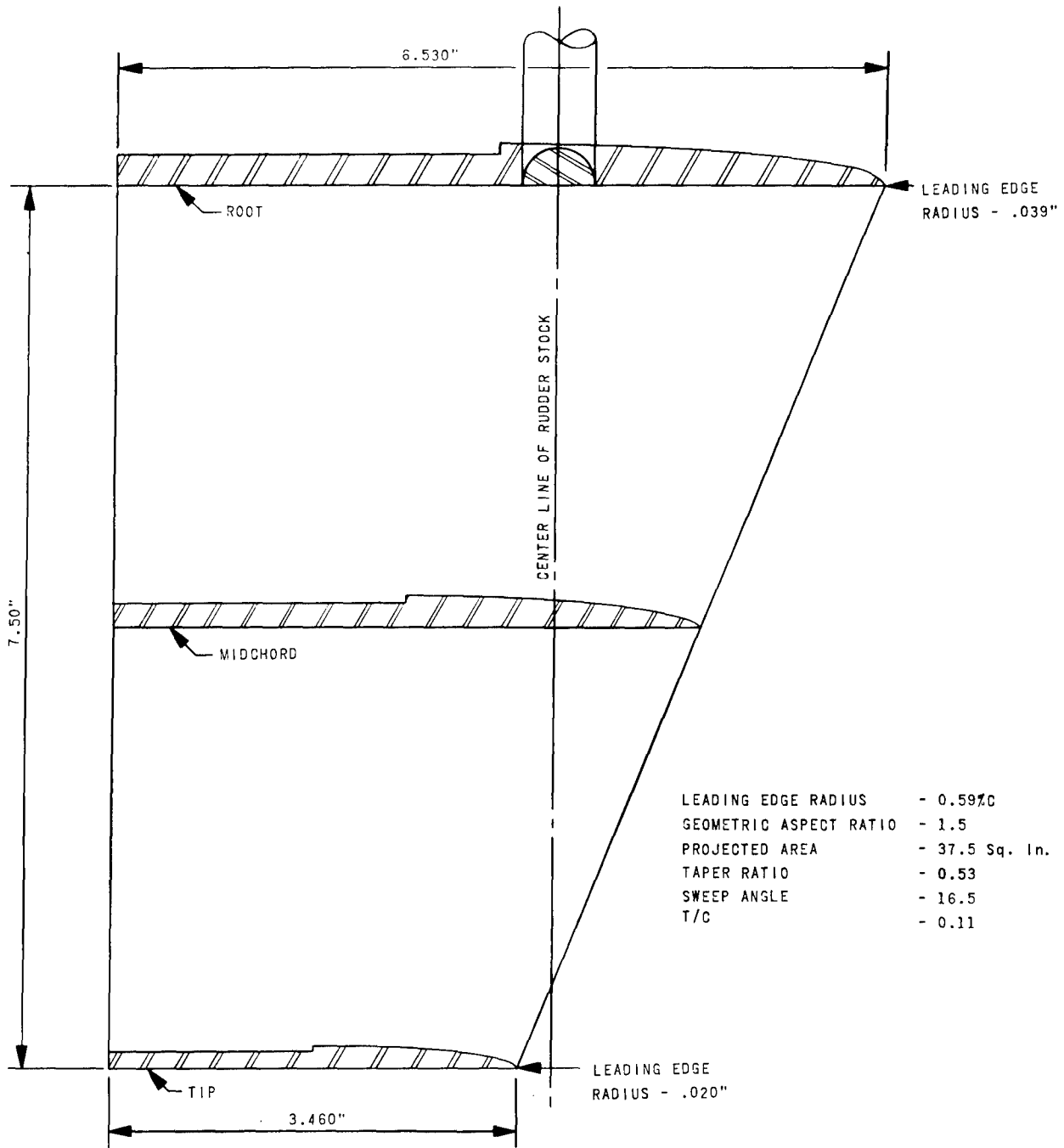
Figure 6 - Planform and Section Details of Rudder 6

14
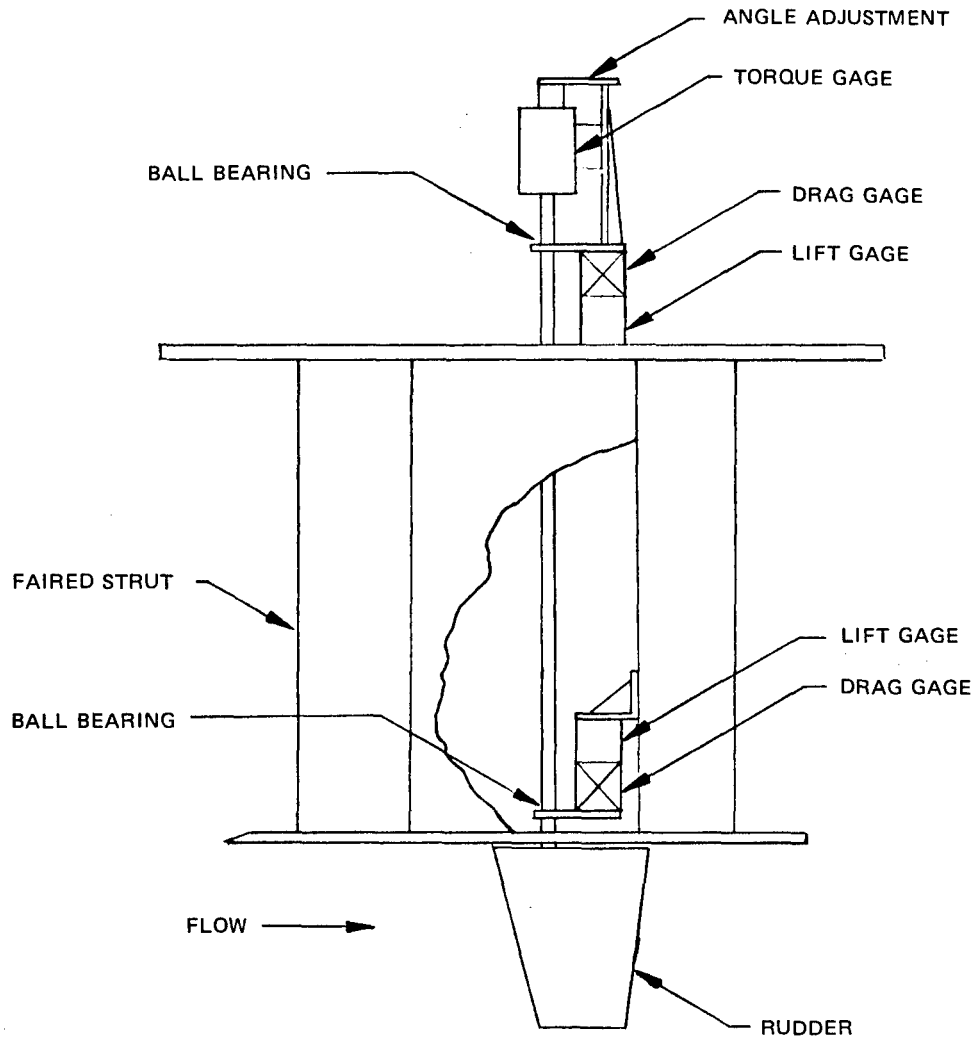
Figure 7 - Details of the Rudder Force Dynamometer Used to Make Force
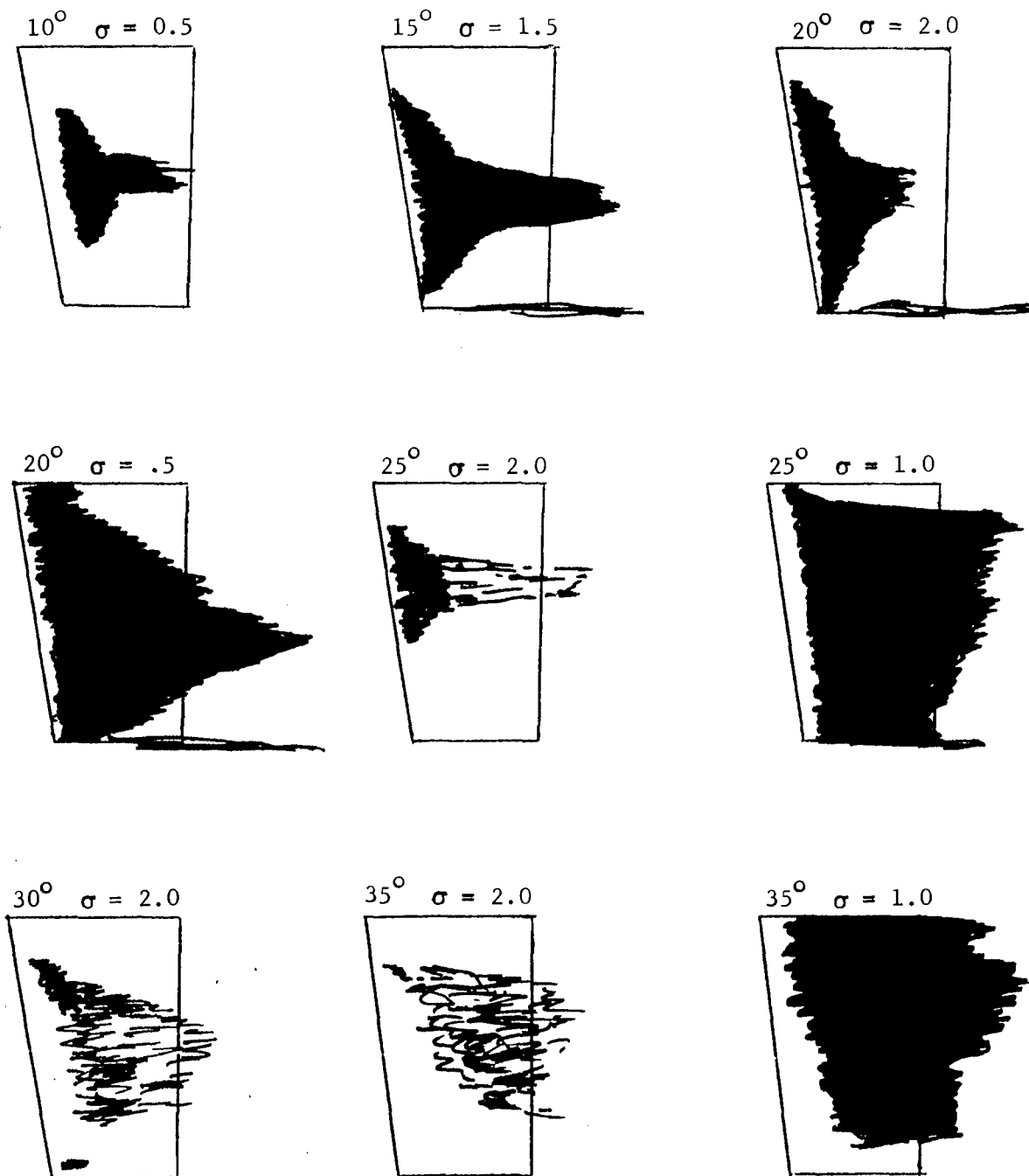Measurements in the 24-Inch Variable-Pressure Water Tunnel

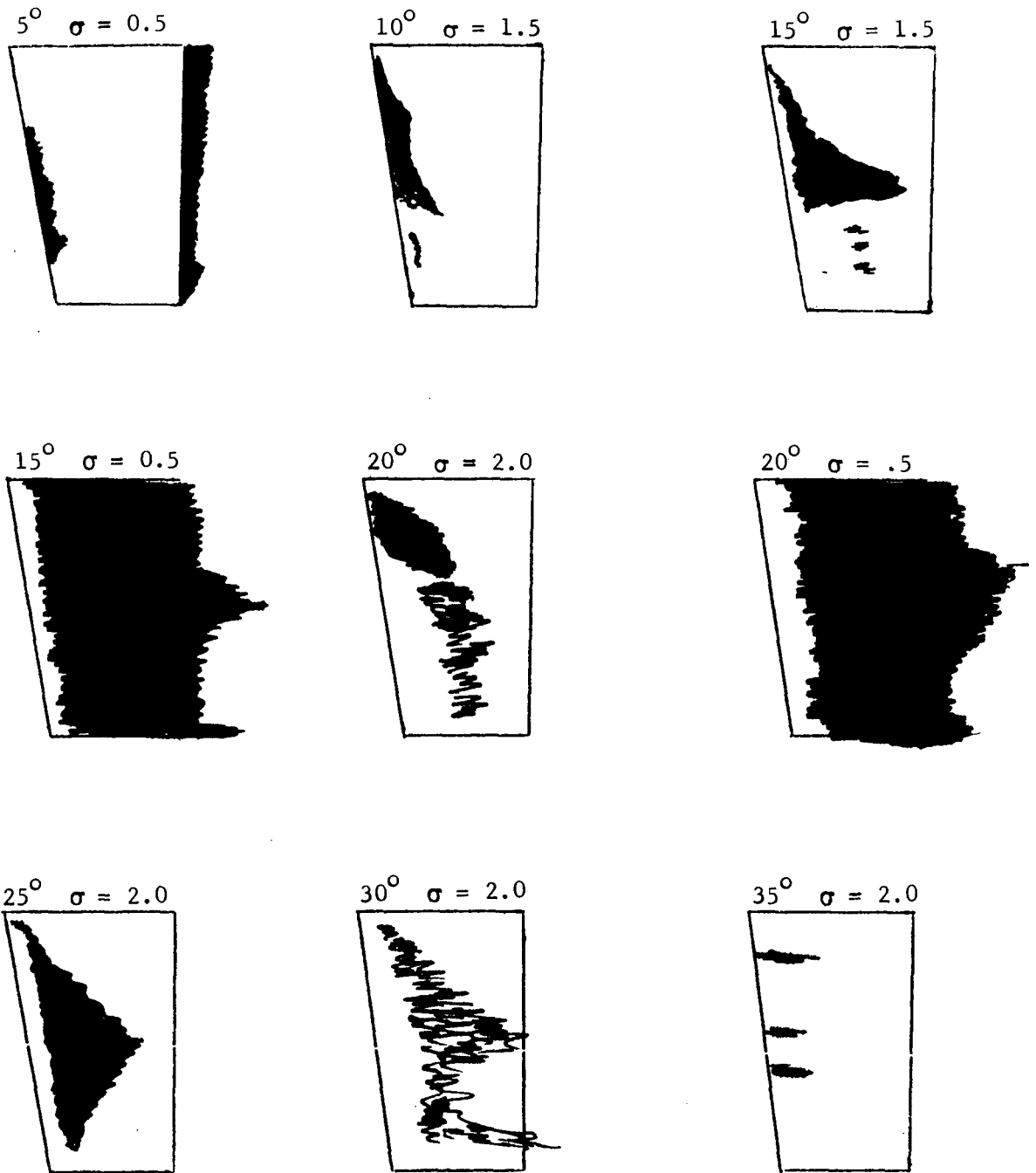Figure 8 - Representative Cavitation Patterns on Rudder 1

5° σ = 0.5   10° σ = 1.5   15° σ = 1.5

15° σ = 0.5   20° σ = 2.0   20° σ = .5

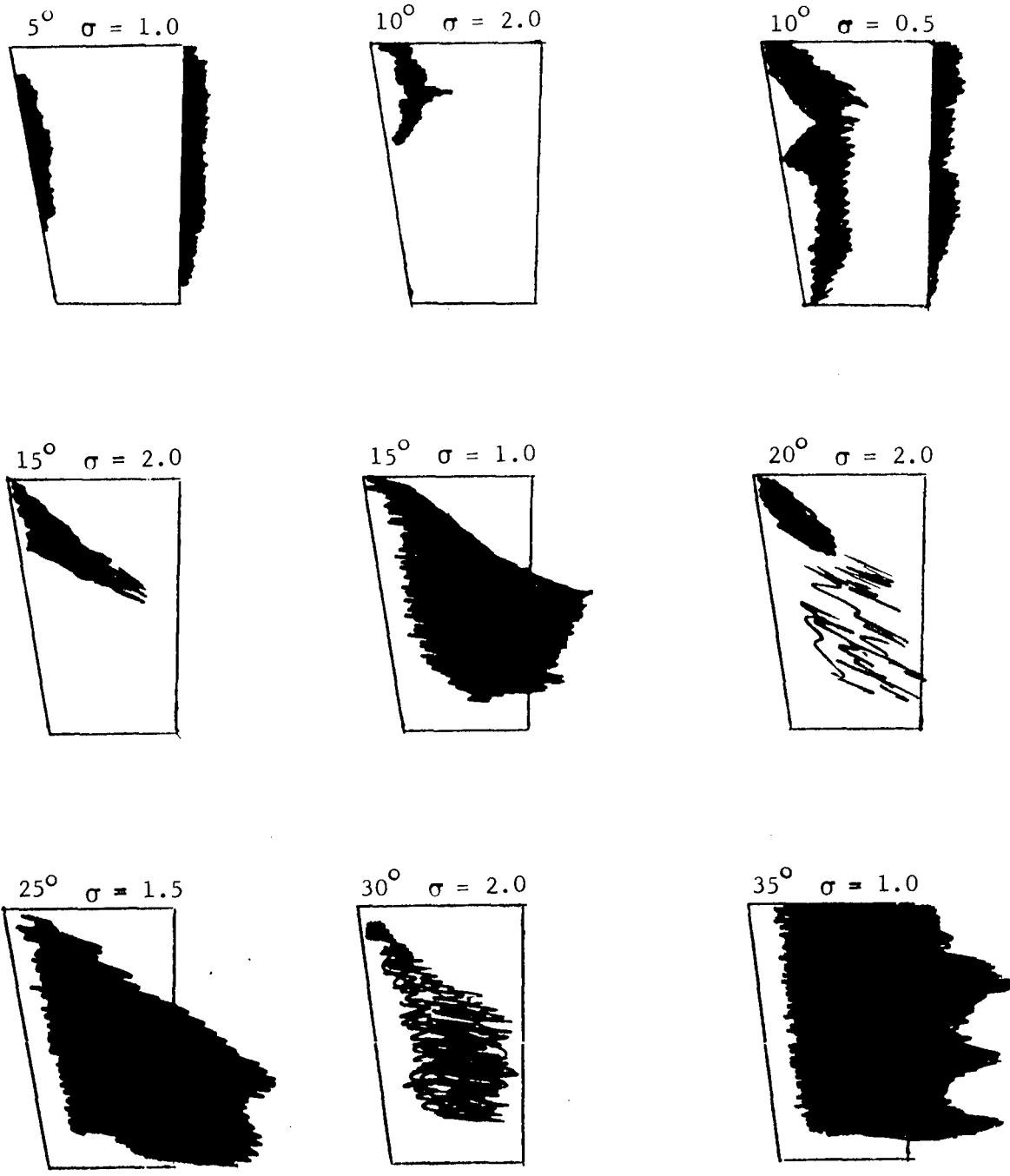25° σ = 2.0   30° σ = 2.0   35° σ = 2.0

Figure 9 - Representative Cavitation Patterns on Rudder 2

17

Figure 10 - Representative Cavitation Patterns on Rudder 3

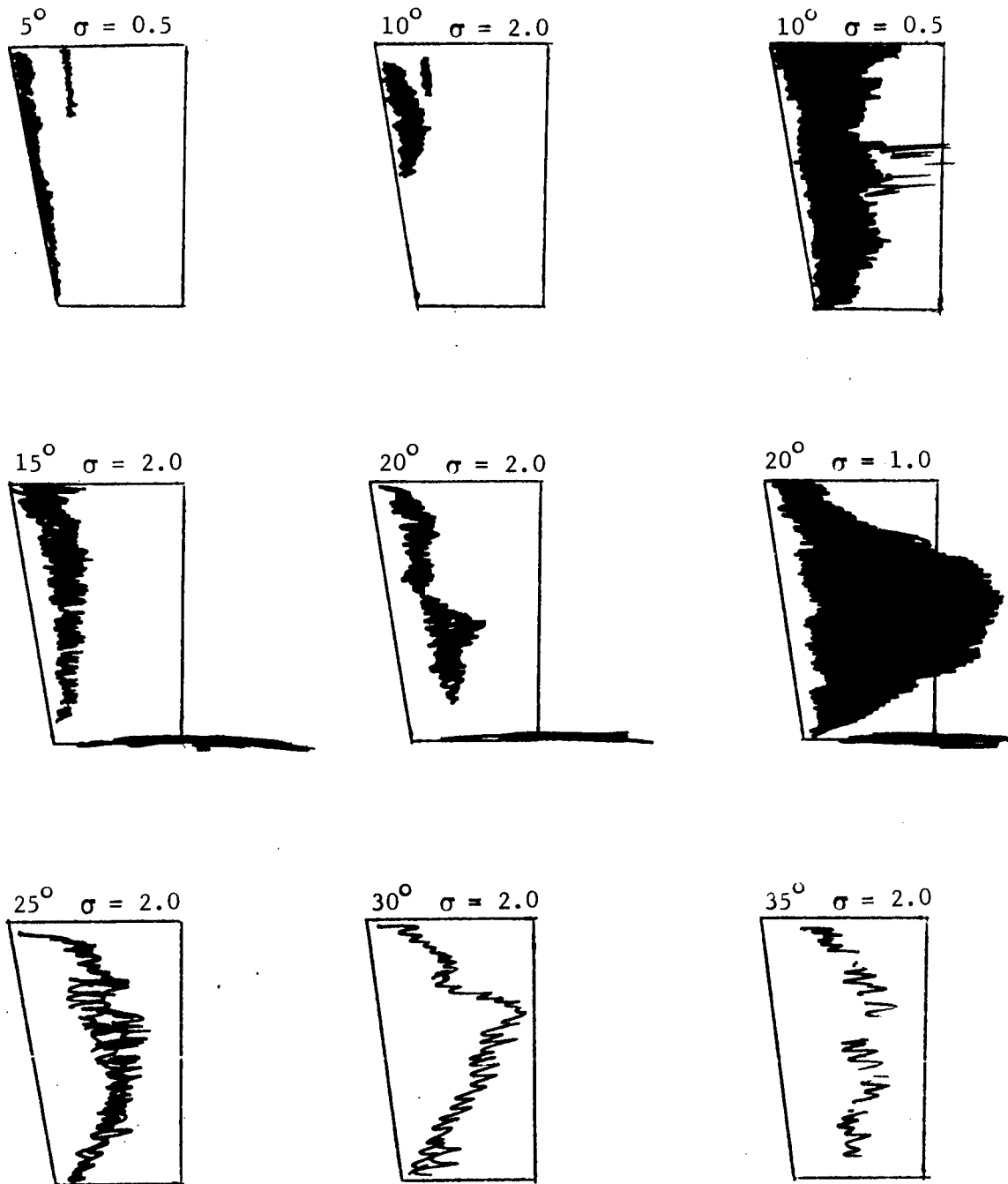Figure 11 - Representative Cavitation Patterns on Rudder 4

5° σ = 0.5   10° σ = 2.0   10° σ = 0.5

15° σ = 2.0   15° σ = 1.0   20° σ = 1.5
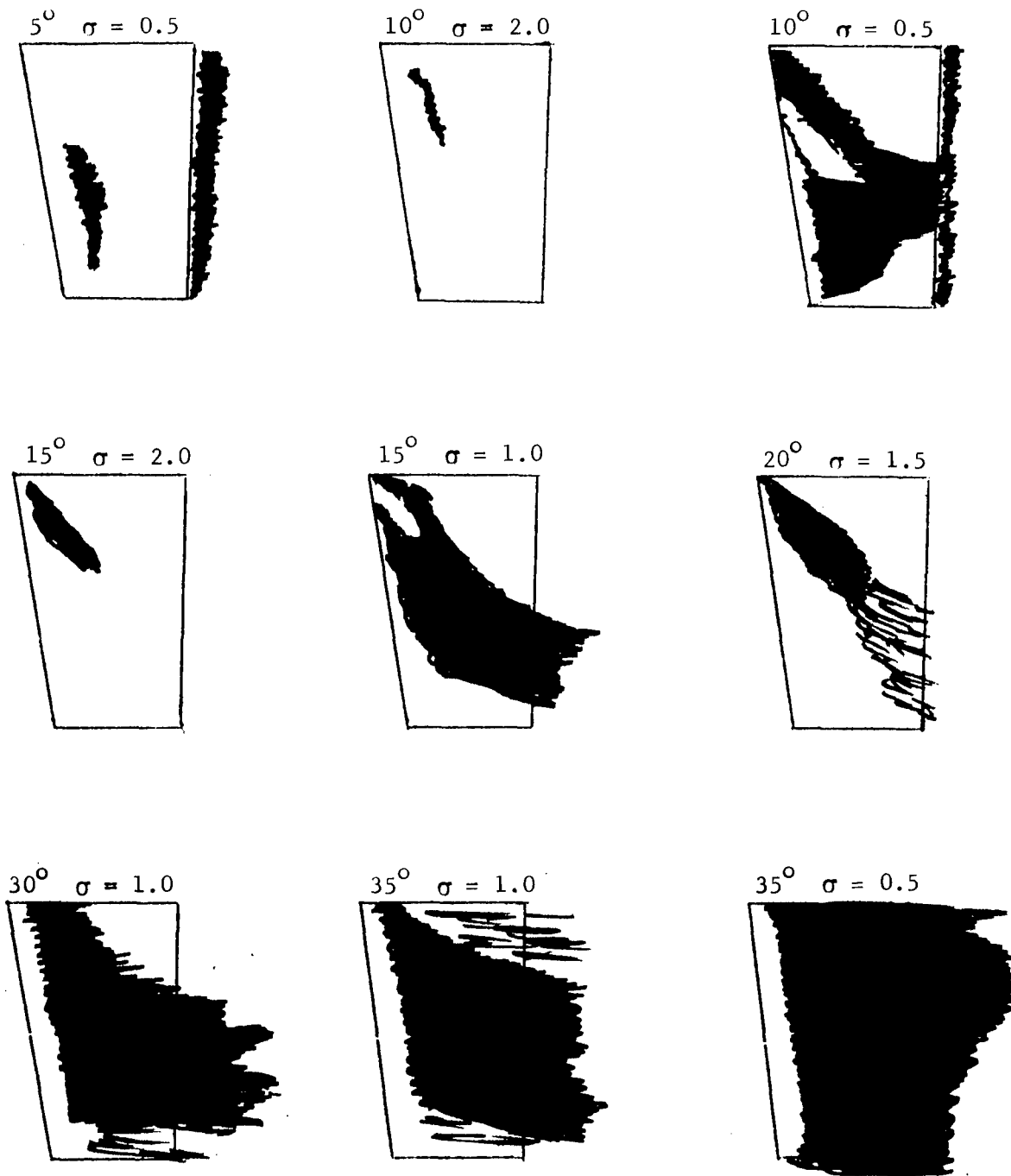
30° σ = 1.0   35° σ = 1.0   35° σ = 0.5

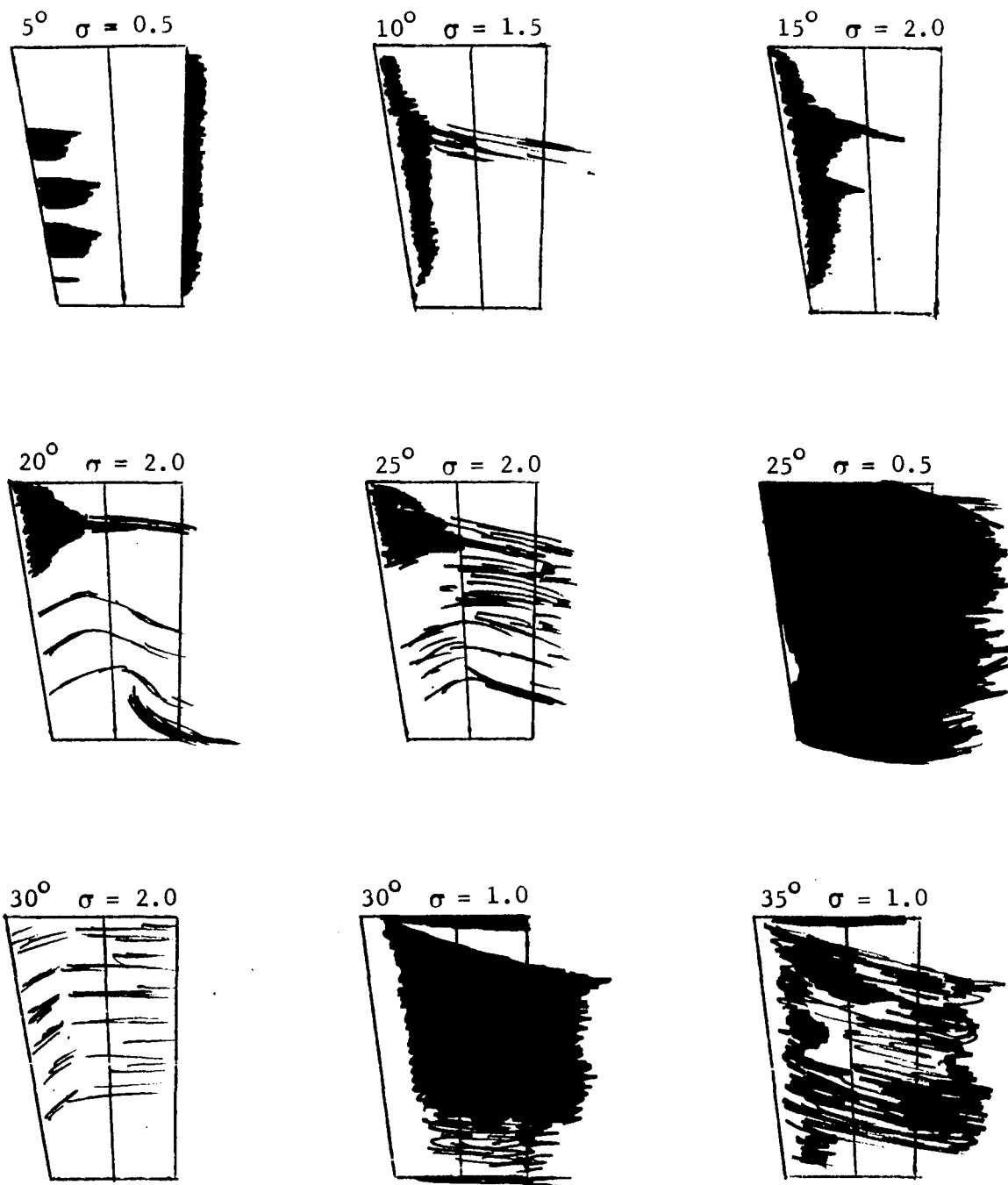Figure 12 - Representative Cavitation Patterns on Rudder 5

Figure 13 - Representative Cavitation Patterns on Rudder 6

Figure 14 – Force and Moment Coefficients Measured on Rudder 1 at Several Rudder Angles and Cavitation Indices

22

Figure 15 – Force and Moment Coefficients Measured on Rudder 2 at Several Rudder Angles and Cavitation Indices
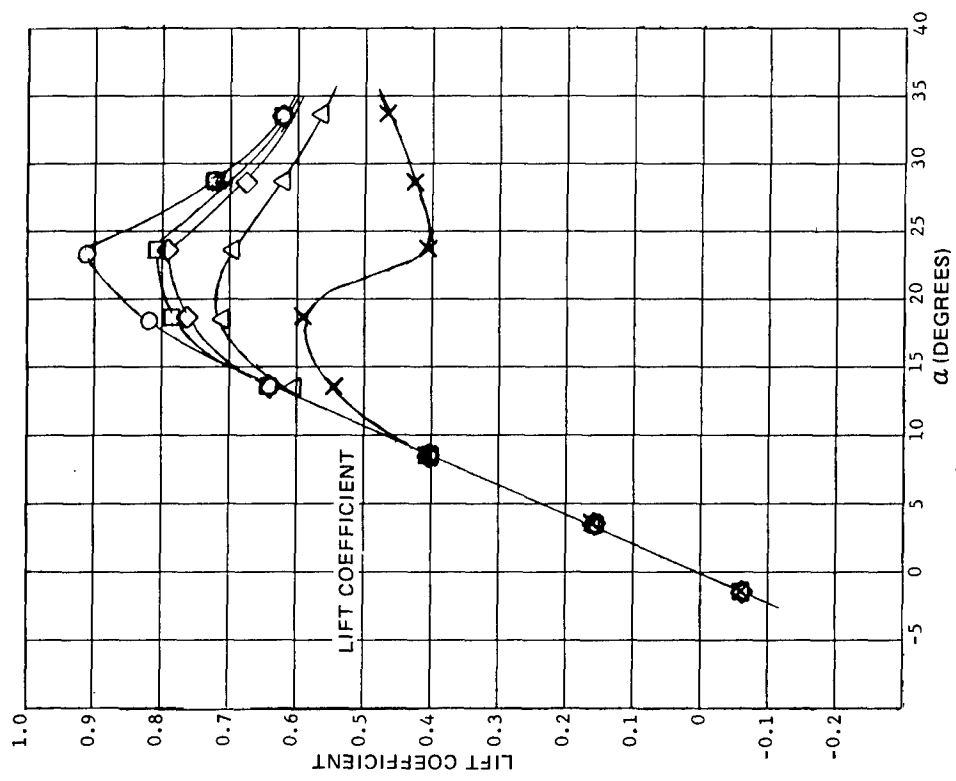
23
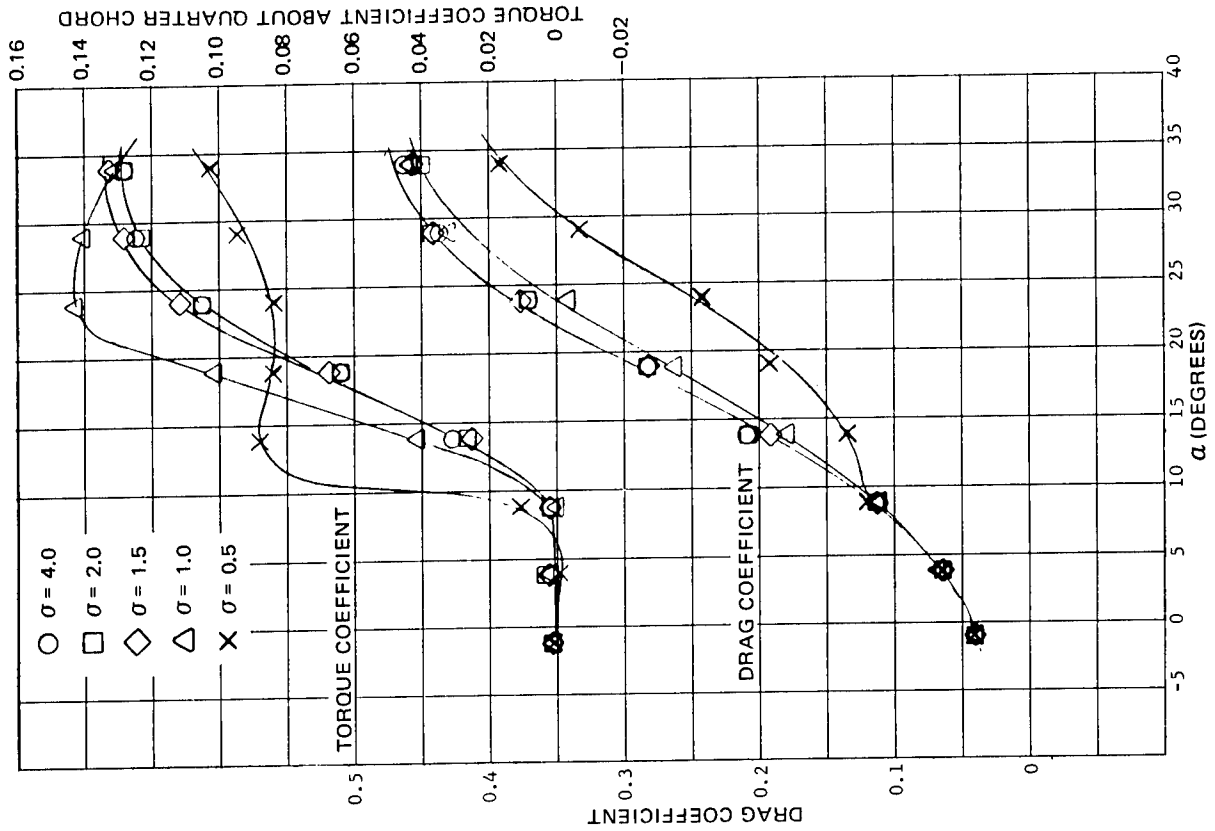
Figure 16 - Force and Moment Coefficients Measured on Rudder 3 at Several
Rudder Angles and Cavitation Indices

24
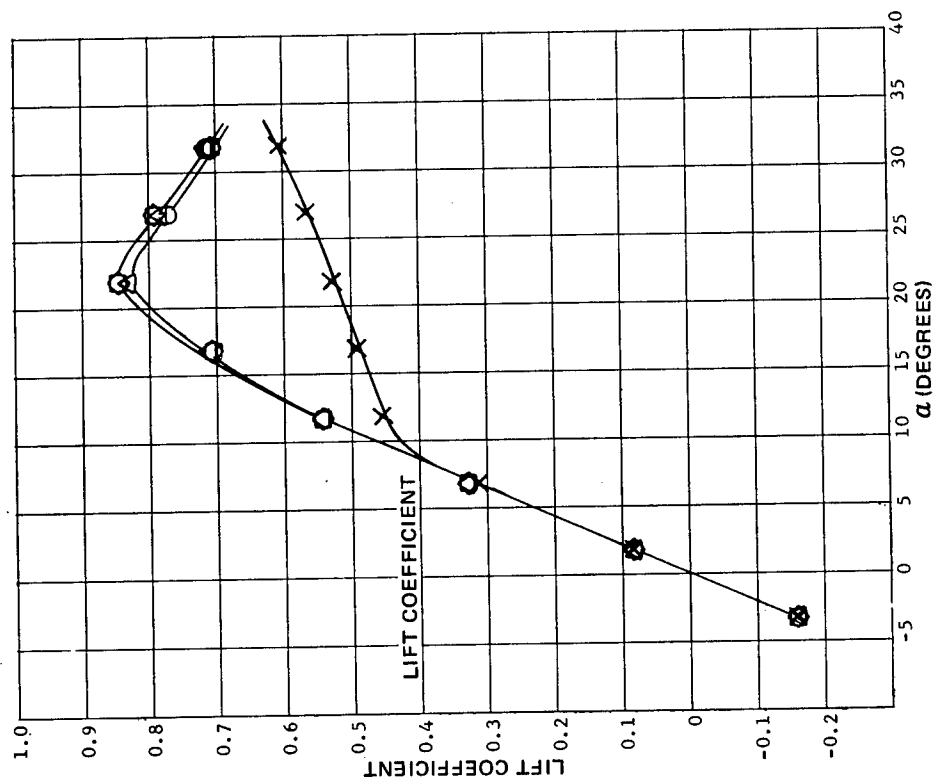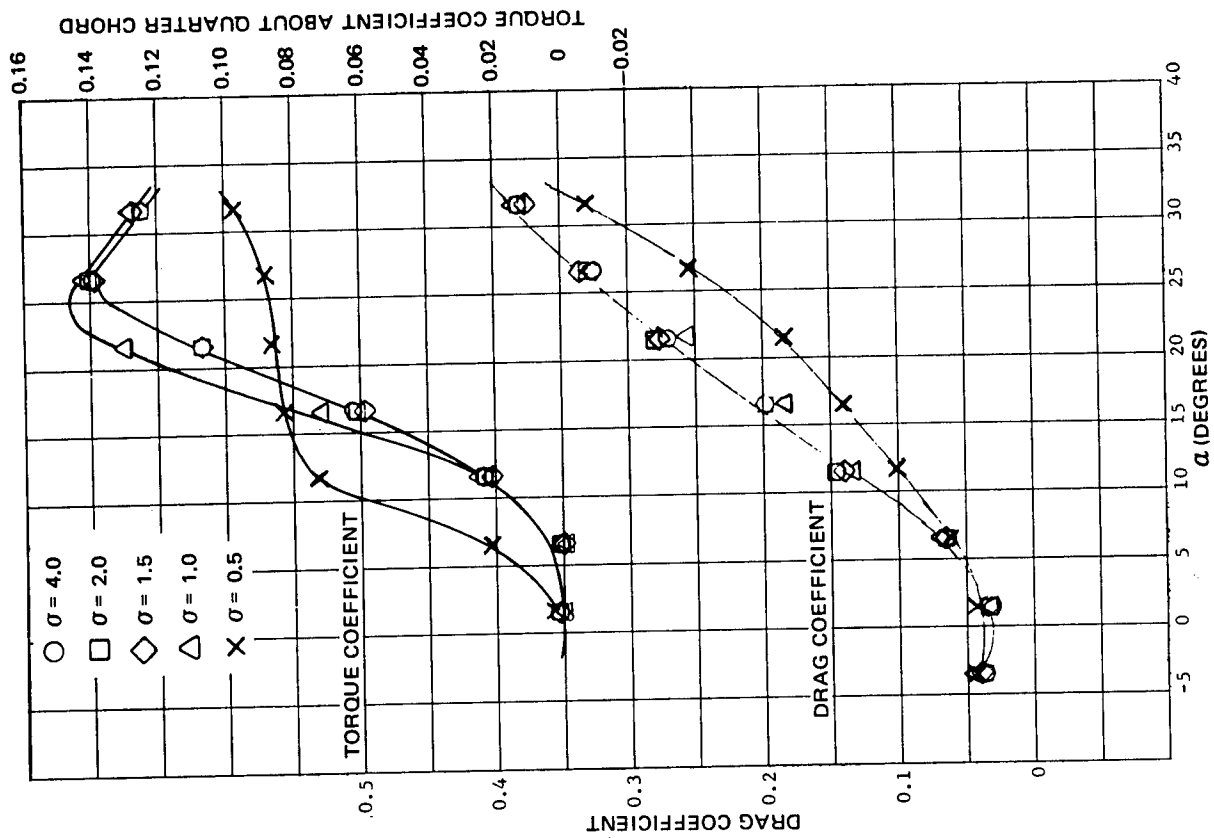
Figure 17 – Force and Moment Coefficients Measured on Rudder 4 at Several
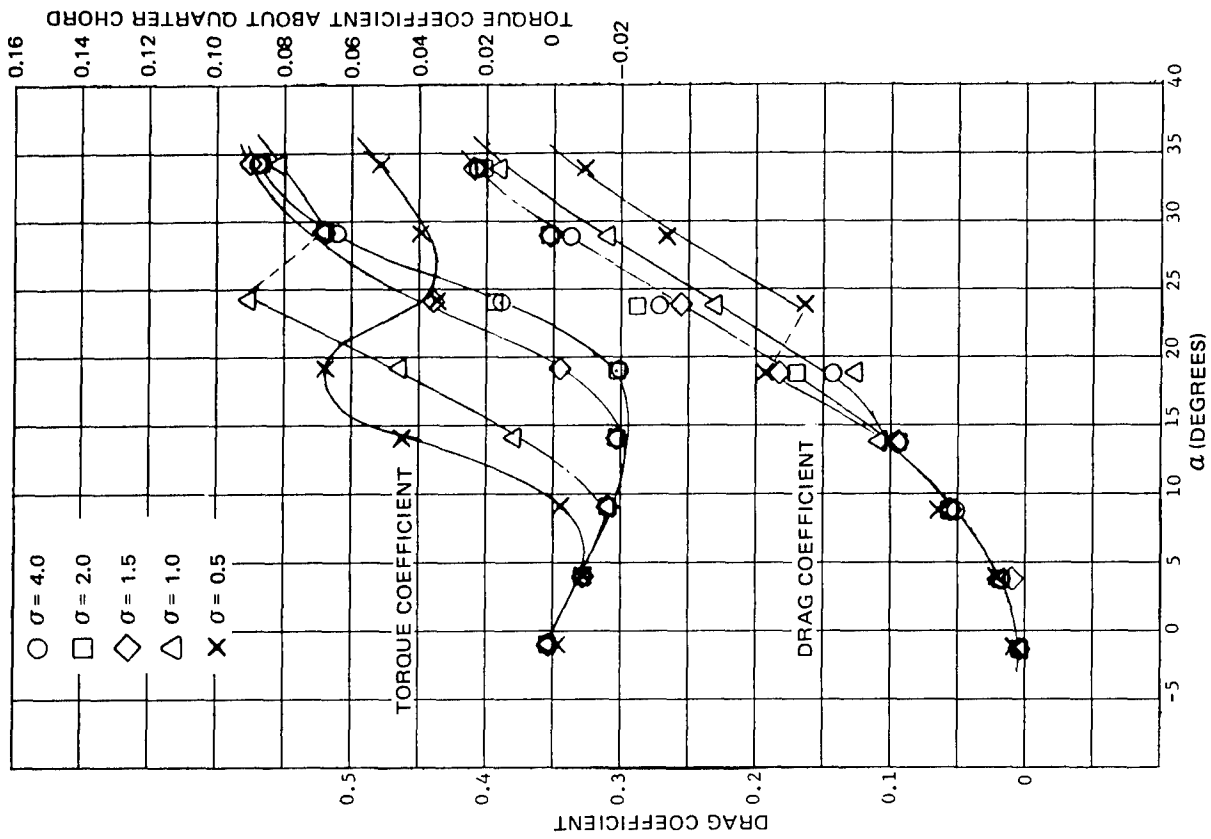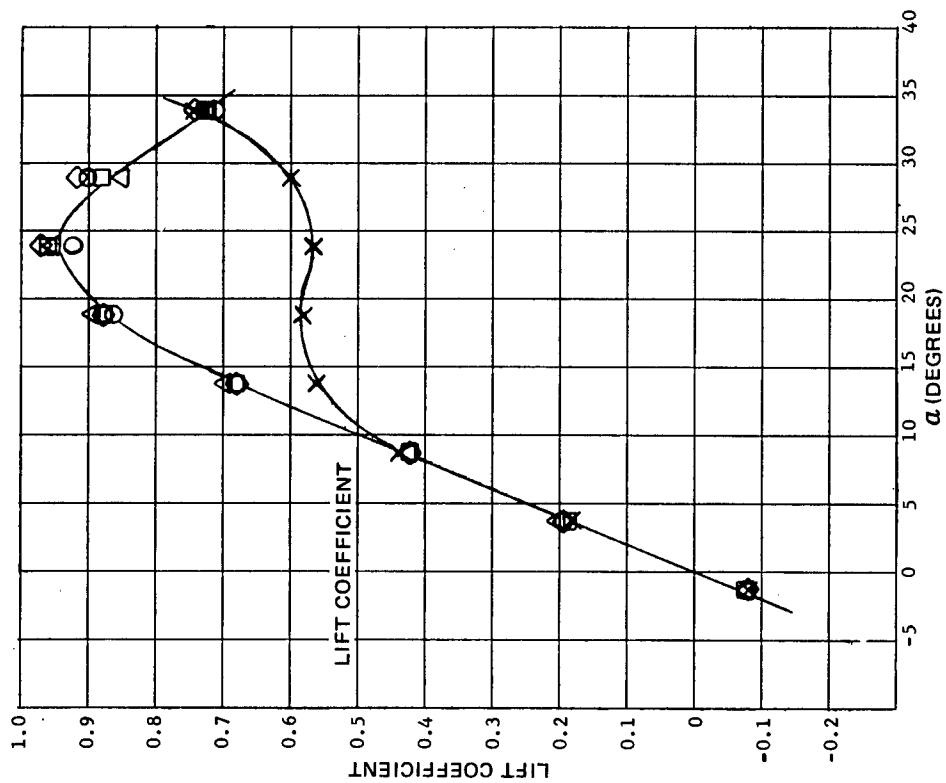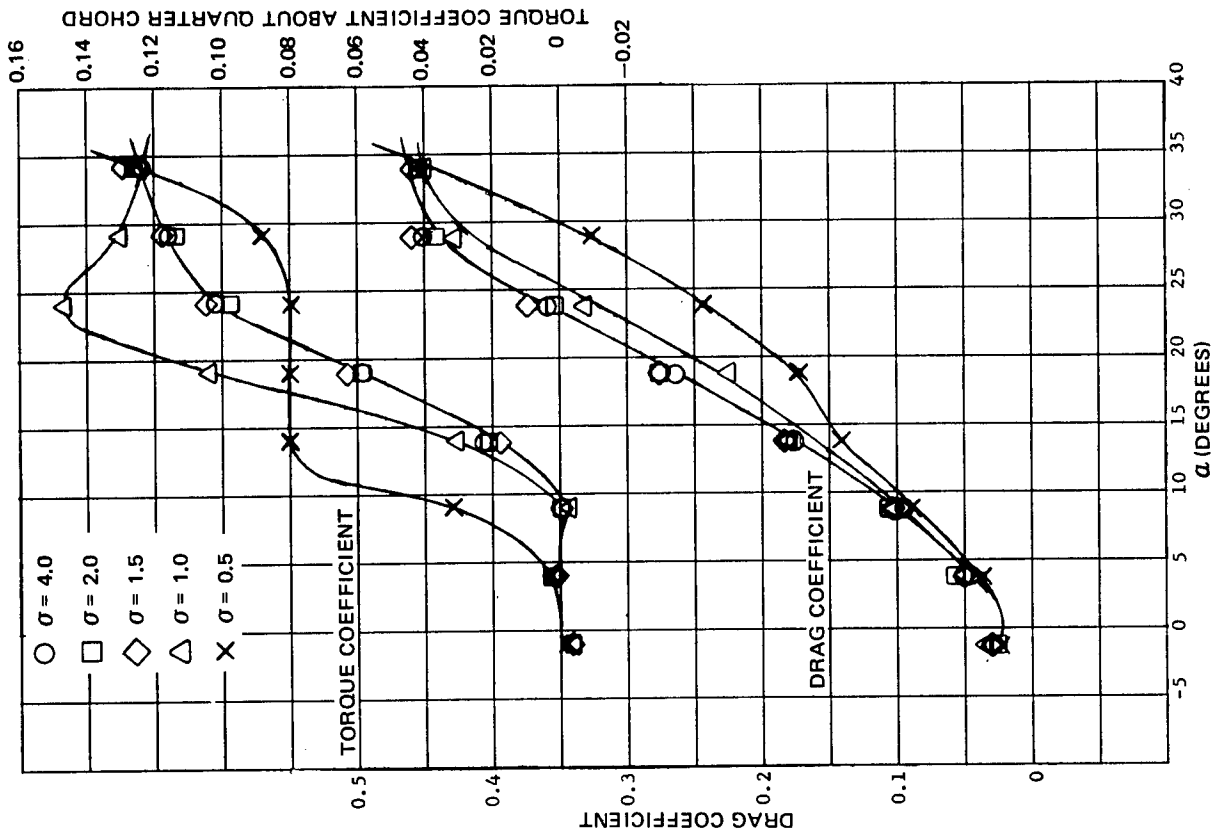Rudder Angles and Cavitation Indices

25
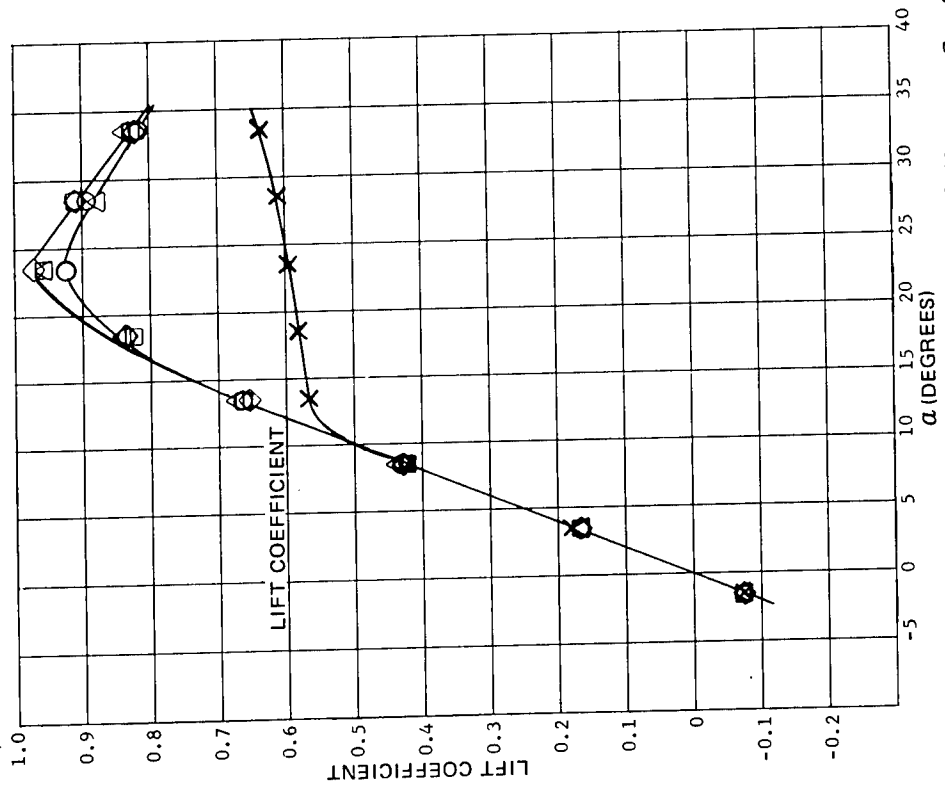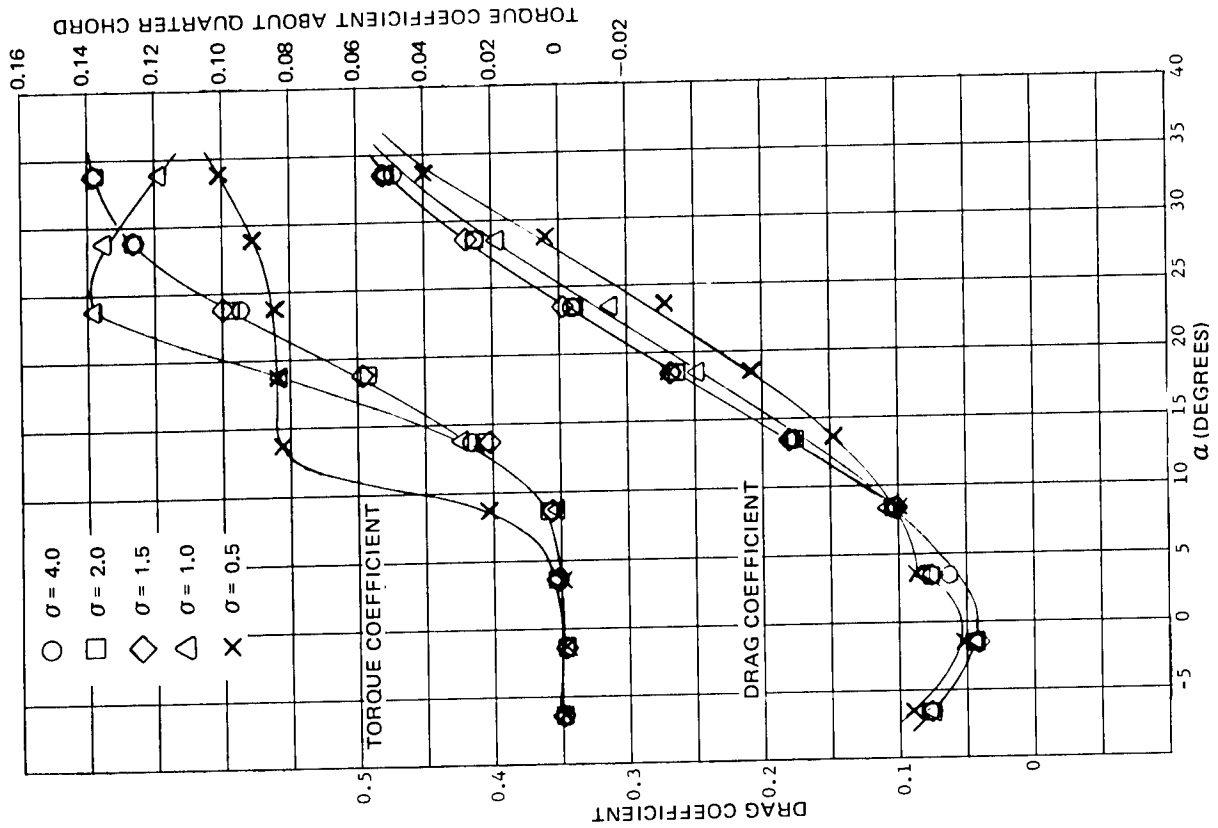
Figure 18 - Force and Moment Coefficients Measured on Rudder 5 at Several
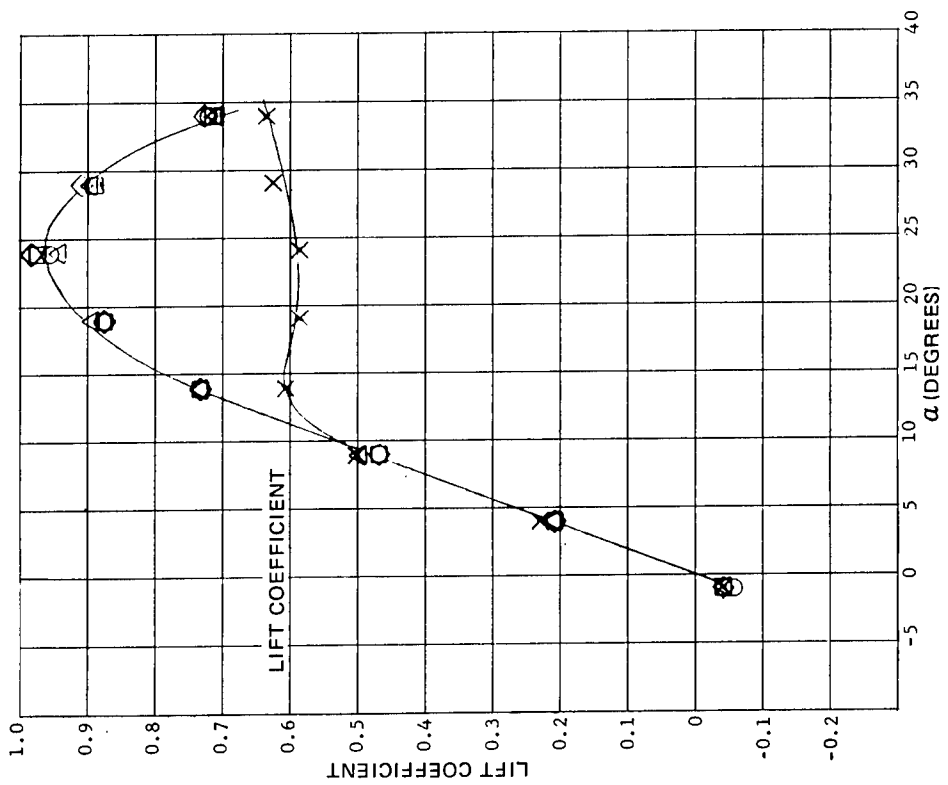Rudder Angles and Cavitation Indices

26
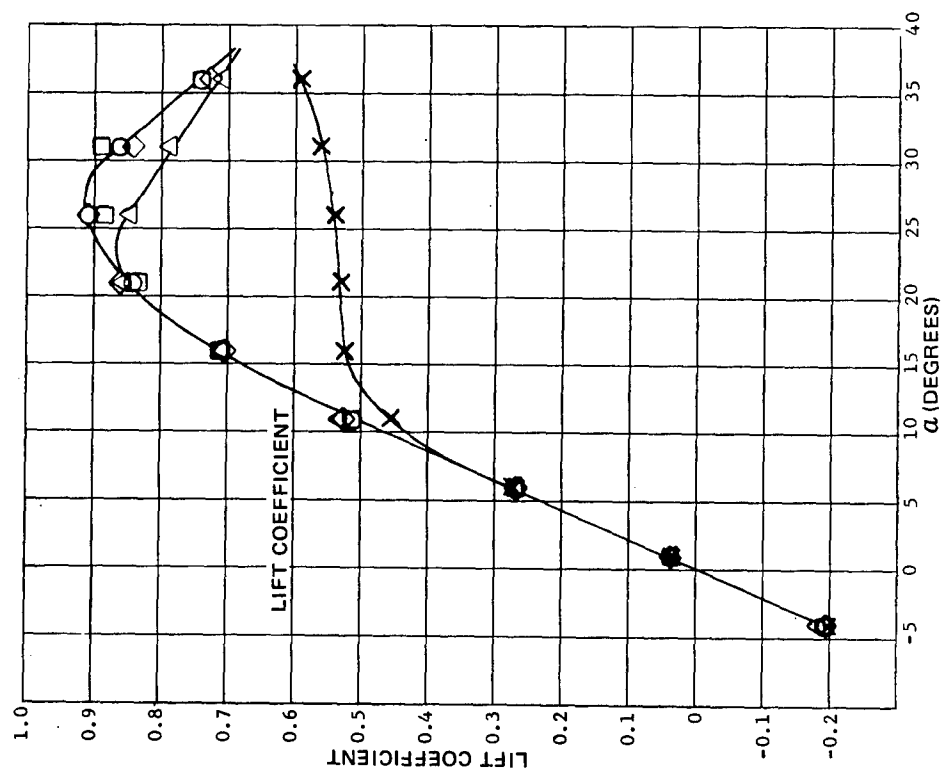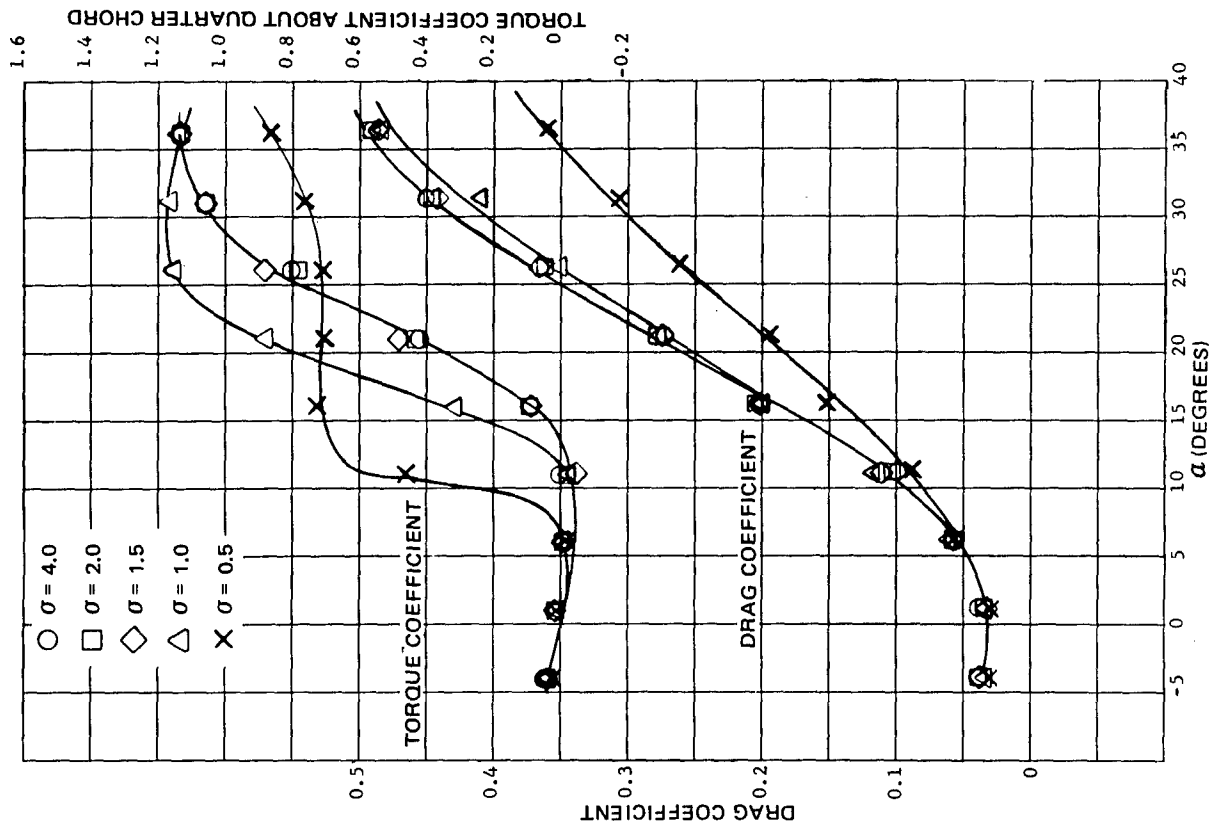
Figure 19 – Force and Moment Coefficients Measured on Rudder 6 at Several
Rudder Angles and Cavitation Indices

27
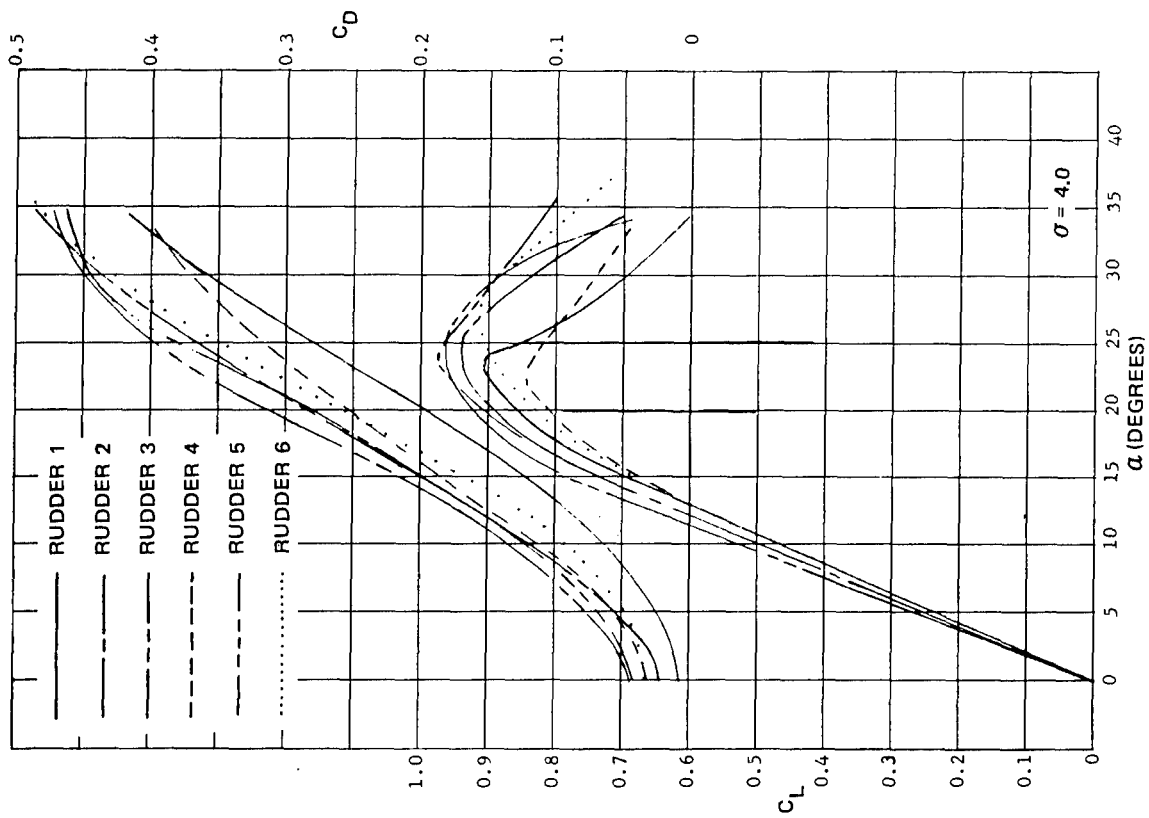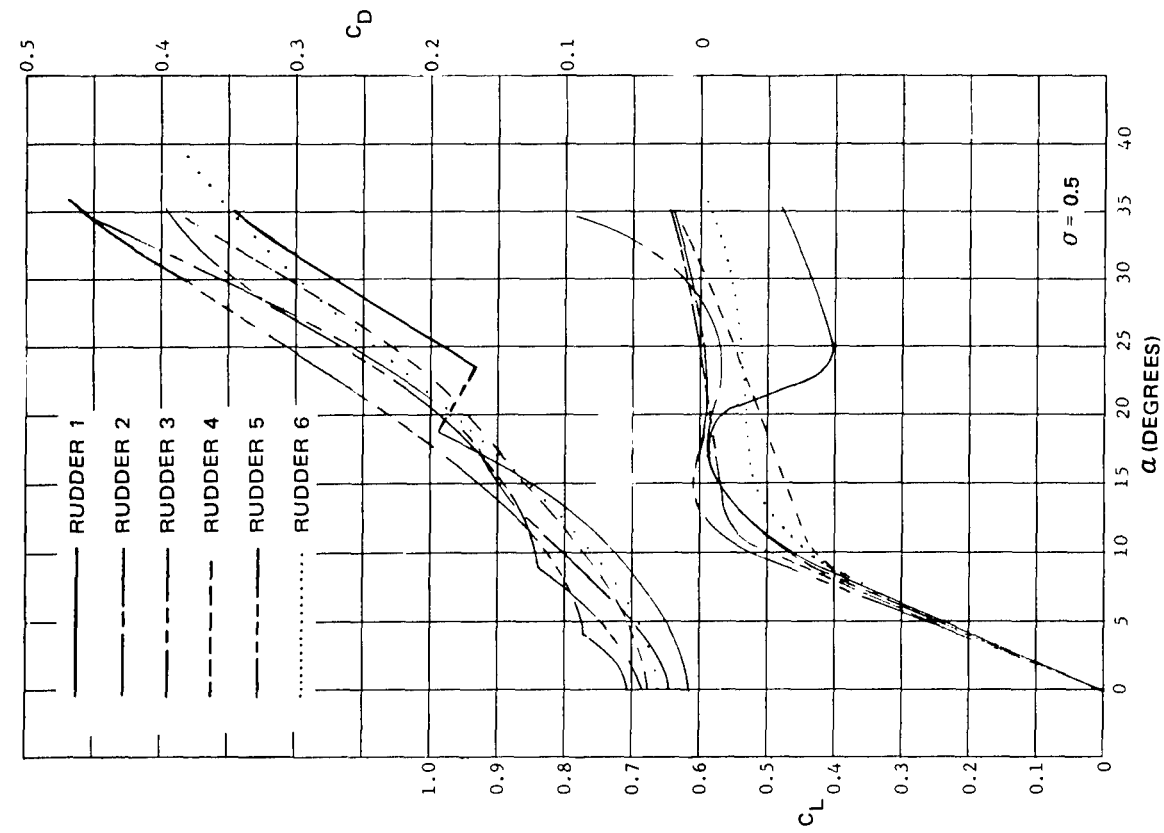
Figure 20 - Comparison of Lift and Drag Coefficients of Rudders 1-6
at Cavitation Indices of 4.0 and 0.5
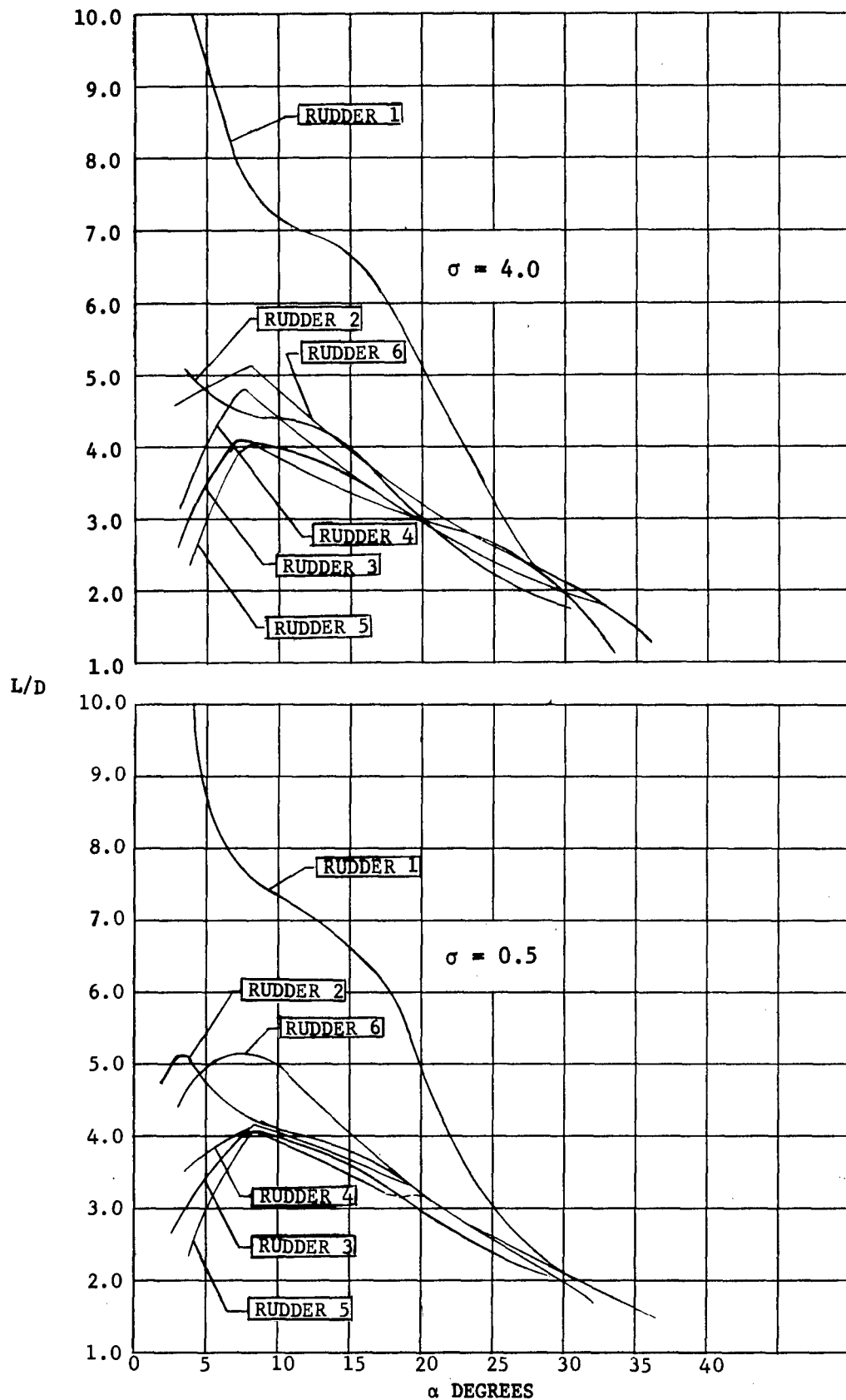
Figure 21 - Comparison of the Lift to Drag Ratios of the Rudders at
Cavitation Indices of 4.0 and 0.5
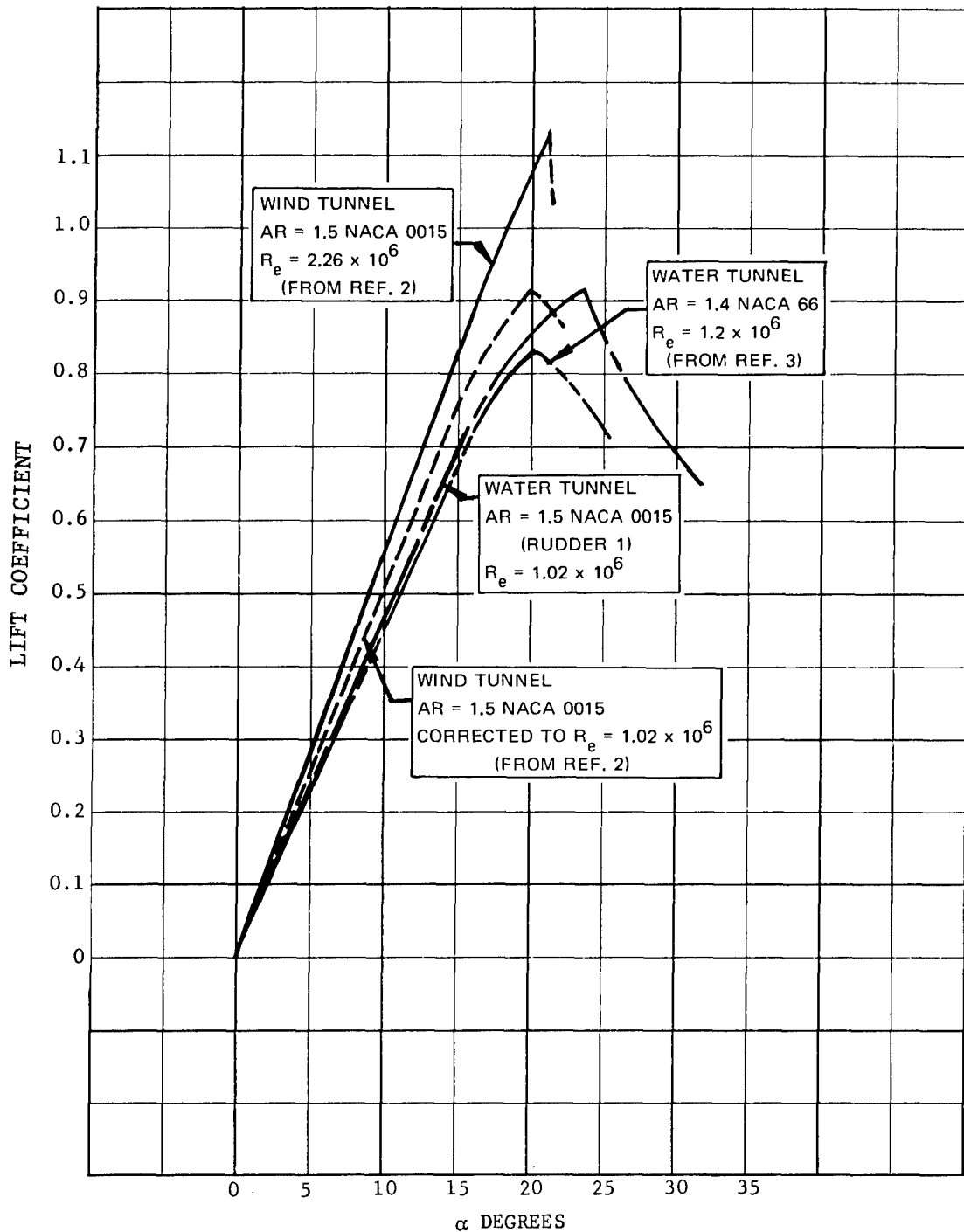
Figure 22 - Comparison of Lift Coefficient versus Angle of Attack for
Rudder 1 as Determined from Wind Tunnel and
Water Tunnel Experiments
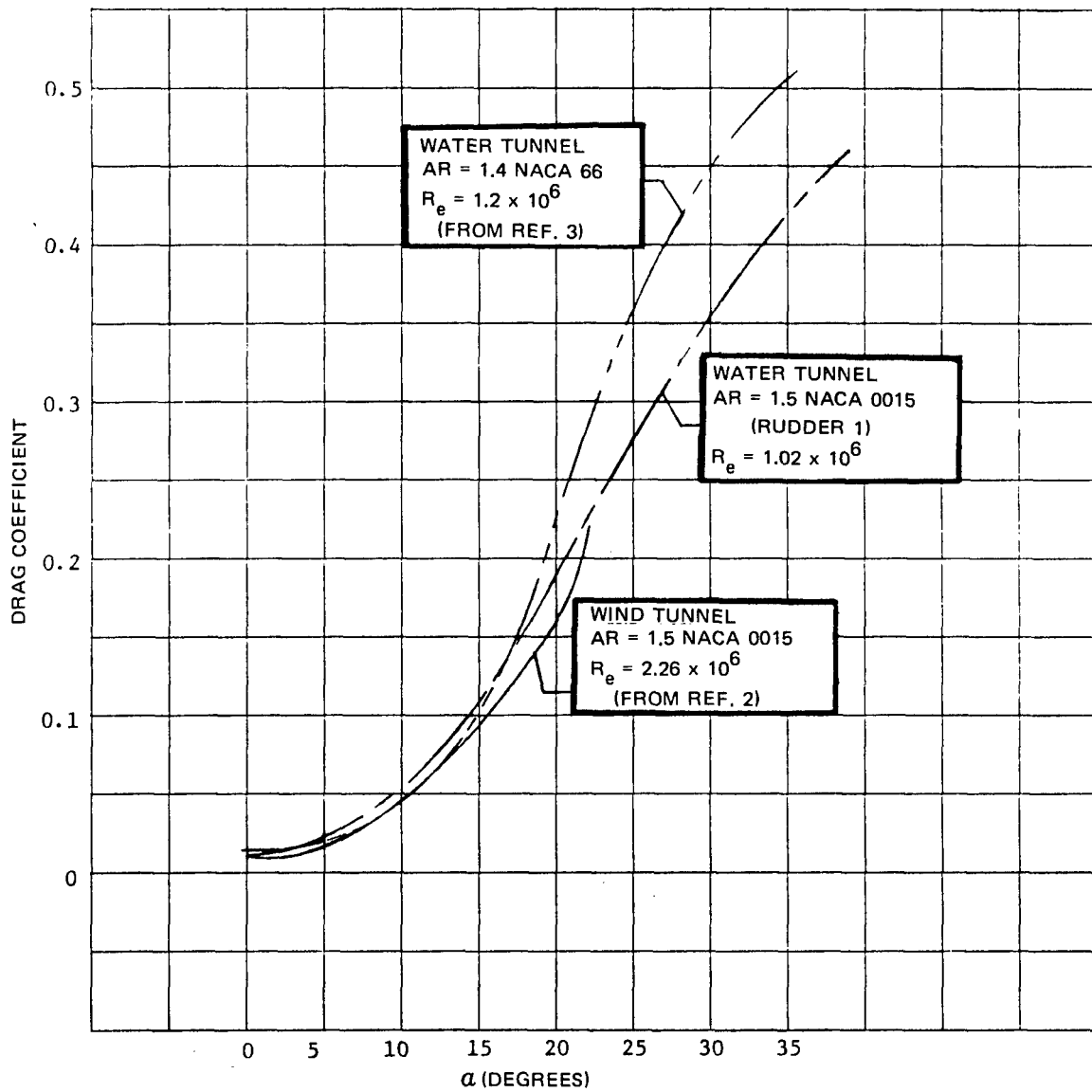
Figure 23 - Comparison of Drag Coefficient versus Angle of Attack for
Rudder 1 as Determined from Wind Tunnel and
Water Tunnel Experiments

```
              INITIAL DISTRIBUTION
              REPORT  4150
    SERIAL

         1            WES/LIBRARY
         2            CHONR 438
         3            ONR BOSTON
         4            ONR CHICAGO
         5            ONR PASADENA
         6            NRL 2627 LIB
         7            USNA LIB
         8            NAVPGSCOL LIB
         9            NROTC & NAVADMINU, MIT
        10            NAVWARCOL
        11            SHIPS 2052
        12            SHIPS 03412/PETERSON
        13            SHIPS 0372
        14            FAC 032C
        15            ORD 035/SEIDMAN
        16            NAVOCEANO 1640
        17            NAVAIRDEVCEN ADL
        18            NELC LIB
        19            NAVWPNSCEN
        20            NAVUSEACEN SAN DIEGO
        21            NAVUSEACEN 6005/FABULA
        22            NAVUSEACEN PASADENA
        23            NAVUSEACEN 2501/HOYT
        24            CIVENGRLAB L31 LIB
        25            NOL
        26            NWL LIB
        27            NPTLAB NUSC
        28            NLONLAB NUSC
        29            NAVSHIPYD BREM/LIB
        30            NAVSHIPYD BSN/LIB
        31            NAVSHIPYD CHASN/LIB
        32            NAVSHIPYD HUNTERS PT/LIB
        33            NAVSHIPYD LBEACH/LIB
        34            NAVSHIPYD MARE/LIB
        35            NAVSHIPYD MARE 250
        36            NAVSHIPYD PEARL/LIB
        37            NAVSHIPYD PHILA 240
        38            NAVSHIPYD PTSMH/LIB
        39            SEC 6034B
        40            SEC 6110
        41            SEC 6114H
        42            SEC 6120
        43            SEC 6136
        44            SEC 6140B/FONCANNON
        45            SEC 6144G
        46            SEC 6148
        47            SEC 6660.03/BLOUNT  NORVA
        48            AFOSR/NAM
        49            DDC
        50            DDC
```

SERIAL

51	DDC
52	DDC
53	DDC
54	DDC
55	DDC
56	DDC
57	DDC
58	DDC
59	DDC
60	DDC
61	LC/SCI & TECH DIV
62	MMA LIB
63	MMA/MARITIME RES CEN
64	DOT LIB
65	U BRIDGEPORT/URAM
66	U CAL BERKELEY/DEPT NAME
67	U CAL NAME/PAULLING
68	U CAL NAME/WEBSTER
69	U CAL NAME/WEHAUSEN
70	U CAL SCRIPPS LIB
71	CIT AERO LIB
72	CIT/ACOSTA
73	CIT/WU
74	CATHOLIC U/HELLER
75	COLORADO STATE U ENGR RES CEN
76	CORNELL U/SEARS
77	FLORIDA ATLANTIC U OE LIB
78	FLORIDA ATLANTIC U/DUNNE
79	U HAWAII/BRETSCHNEIDER
80	U IOWA INST HYDR RES LIB
81	U IOWA IHR/KENNEDY
82	U IOWA IHR/LANDWEBER
83	LEHIGH U FRITZ ENGR LAB LIB
84	LONG ISLAND U/PRICE
85	MIT OCEAN ENGR LIB
86	MIT OCEAN ENGR/ABKOWITZ
87	MIT OCEAN ENGR/MANDEL
88	MIT OCEAN ENGR/NEWMAN
89	U MICHIGAN NAME LIB
90	U MICHIGAN NAME/COUCH
91	U MICHIGAN NAME/HAMMITT
92	U MICHIGAN NAME/OGILVIE
93	U MICHIGAN WILLOW RUN LABS
94	U MINNESOTA SAFHL/KILLEN
95	U MINNESOTA SAFHL/SCHIEBE
96	U MINNESOTA SAFHL/SONG
97	U MINNESOTA SAFHL/WETZEL
98	NOTRE DAME ENGR LIB
99	NOTRE DAME/STRANDHAGEN
100	SWRI APPLIED MECH REVIEW

SERIAL

101	SWRI/ABRAMSON
102	STANFORD U CIV ENGR LIB
103	STANFORD U/STREET
104	STANFORD RES INST LIB
105	SIT DAVIDSON LAB LIB
106	SIT DAVIDSON LAB/BRESLIN
107	SIT DAVIDSON LAB/TSAKONAS
108	U WASHINGTON APL LIB
109	WEBB INST/LEWIS
110	WEBB INST/WARD
111	WHOI OCEAN ENGR DEPT
112	WPI ALDEN HYDR LAB LIB
113	SNAME
114	BETHLEHEM STEEL NEW YORK/LIB
115	BETHLEHEM STEEL SPARROWS
116	BOLT BERANEK AND NEWMAN LIB
117	EASTERN RES GROUP
118	ESSO DES DIV
119	GEN DYN ELEC BOAT/BOATWRIGHT
120	GIBBS & COX
121	HYDRONAUTICS LIB
122	HYDRONAUTICS/GERTLER
123	LOCKHEED M&S/WAID
124	DOUGLAS AIRCRAFT/SMITH
125	NEWPORT NEWS SHIPBUILDING LIB
126	NIELSEN ENGR/SPANGLER
127	NAR SPACE/UJIHARA
128	OCEANICS/
129	SPERRY SYS MGMT LIB
130	SUN SHIPBUILDING AERO/HYDRO
131	ROBERT TAGGART
132	TRACOR

CENTER DISTRIBUTION

SERIAL

133	C	1500	CUMMINS WILLIAM E
134	C	1502	STUNTZ GEORGE R JR
135	C	1520	WERMTER RAYMOND
136	C	1524	WILSON CHARLES J
137	C	1524	WILSON CHARLES J
138	C	1532	DOBAY GABOR F
139	C	1532	GREGORY DOUGLAS L
140	C	1540	MORGAN WILLIAM B
141	C	1560	HADLER JACQUES B
142	C	1572	OCHI MARGARET D

DOCUMENT CONTROL DATA - R & D

Security classification of title, body of abstract and indexing annotation must be entered when the overall report is classified)

1 ORIGINATING ACTIVITY (Corporate author)	2a. REPORT SECURITY CLASSIFICATION
Naval Ship Research and Development Center Bethesda, Md. 20034	UNCLASSIFIED
	2b. GROUP

3 REPORT TITLE

FORCE AND MOMENT CHARACTERISTICS OF SIX HIGH-SPEED RUDDERS FOR USE ON HIGH-PERFORMANCE CRAFT

4. DESCRIPTIVE NOTES (Type of report and inclusive dates)

5. AUTHOR(S) (First name, middle initial, last name)

Douglas L. Gregory

6. REPORT DATE	7a. TOTAL NO. OF PAGES	7b. NO. OF REFS
November 1973	39	3

8a. CONTRACT OR GRANT NO.	9a. ORIGINATOR'S REPORT NUMBER(S)
Program Element 62512N	
b. PROJECT NO. F35421 Subproject SF 35421006	4150
c. Work Unit 1532-100	9b. OTHER REPORT NO(S) (Any other numbers that may be assigned this report)
d.	

10. DISTRIBUTION STATEMENT

APPROVED FOR PUBLIC RELEASE: DISTRIBUTION UNLIMITED

11. SUPPLEMENTARY NOTES	12. SPONSORING MILITARY ACTIVITY
	Naval Ship Systems Command Code 03412B

13. ABSTRACT

Six rudders with a geometric aspect ratio of 1.5 and widely varying section shapes were constructed to determine the effect of section shape on the cavitating performance of high-speed rudders. Experiments were conducted in the 24-in. variable-pressure water tunnel at cavitation indices between 4.0 and 0.5 and an angle of attack range from -5 to +35 deg. Section shape had little effect on the lift curve slope or on the maximum lift coefficient. However, the blunt base sections had substantially higher drag coefficients throughout the normal operating range of rudder angles. Rudder stock torque was significantly affected by section shape and cavitation index.

14 KEY WORDS	LINK A		LINK B		LINK C	
	ROLE	WT	ROLE	WT	ROLE	WT
High-Performance Craft						
Rudder Forces under Cavitating Conditions						
Water Tunnel Data						
Wind Tunnel Data						

DD _{1 NOV 65} **1473** (BACK)

(PAGE 2)